SLAG AS A HEAT TRANSFER MEDIUM

by

HAROLD ALAN FINE

B.S., Carnegie-Mellon University
(1969)

M.S., Carnegie-Mellon University
(1969)

Submitted in partial fulfillment of the requirements

for the degree of

DOCTOR OF SCIENCE

at the

Massachusetts Institute of Technology

June, 1973

Signature redacted

Signature of Author . . . .
Department of Metallurgy and Materials Science
May 4, 1973

Signature redacted

Certified by . . . .
Thesis Supervisor

Signature redacted

Accepted by . . . .
Chairman, Departmental Committee on Graduate Students

ABSTRACT

SLAG AS A HEAT TRANSFER MEDIUM

by

HAROLD ALAN FINE

Submitted to the Department of Metallurgy and Materials Science on May 4, 1973 in partial fulfillment of the requirements for the degree of Doctor of Science.

The slag in metallurgical operations may participate to an appreciable extent in the heat transfer processes occurring within the system. Heat transfer in liquid slag at high temperatures can occur by convection, conduction and radiation. It is the purpose of the investigation reported here to study combined conduction and radiation in glasses similar in composition to metallurgical slags.

A new periodic steady-state method is presented for measuring the thermal diffusivity of liquid oxides for temperatures up to 1500°C. A cylindrical glass sample is held in a small thin-walled ingot-iron tube. A molybdenum wire is positioned axially within the tube. The thermal diffusivity of the specimen is obtained by measuring the phase shift between a periodic current impressed on the wire and the temperature reponse at the outer wall of the iron tube. At the high temperatures of the measurements, it is necessary also to consider heat transfer by radiation within the glass. The monochromatic absorption coefficients were measured for the visible and infrared spectra at room temperature for several glass compositions. It was found that the radiation heat transfer within the sample could be described accurately by the diffusion approximation. Consequently, the measured values were the diffusivities for combined radiation and conduction occurring within the melt, and were equal to the "effective thermal diffusivities" of the glasses.

The results of the measurements performed on glasses containing between 11.9 wt. % FeO and 20.9 wt. % FeO and with a lime to silica ratio, B, equal to 1.0 and 1.5 can be represented by the equation

$$k_{eff} \times 10^3 \ (cm^2/sec) = 2.38 \ (1.5 - 0.5 \ B) + 200.7 \ \frac{(T/1500)^3}{(\% \ FeO)^2}$$

with an associated error of ±10%. The relative importance of the thermal conductivity and the radiation conductivity to the total heat transfer process was also determined for the investigated glasses. The thermal and radiation conductivities were found to be of the same order of magnitude.

A surface renewal model is also proposed to describe the role of convection in a liquid slag layer of an electric furnace. The practical implications of this model are discussed.

Thesis Supervisor: John F. Elliott
            Title: Professor of Metallurgy

TABLE OF CONTENTS

TABLE OF CONTENTS (cont'd)

TABLE OF CONTENTS (cont'd)

LIST OF FIGURES AND ILLUSTRATIONS

LIST OF FIGURES AND ILLUSTRATIONS (cont'd)

LIST OF TABLES

NOMENCLATURE

a	constant
A	area
A_T	amplitude attenuation coefficient
$AL...AW$	constants
b	constant
B	lime to silica ratio
$BL...BW$	constants
C_m	concentration
C_p	heat capacity
C_{pi}	heat capacity of component i
C_2	constant
$e_{b\lambda}$	monochromatic black body emissive power
E_λ	monochromatic extinction coefficient
f	frequency
F	mean free path of a photon
F_{i-j}	configuration factor between i and j
g	gravitational constant
h	heat transfer coefficient
h_r	linearized radiation heat transfer coefficient
i'_λ	directional monochromatic intensity
I_λ	monochromatic intensity
$J_i(z)$	Bessel function of the first kind of order i
k_c	thermal diffusivity

k_r	radiation diffusivity
k_{eff}	effective thermal diffusivity
K	constant
K_c	thermal conductivity
K_{eff}	effective thermal conductivity
K_r	radiation conductivity
L	mean free path of a phonon
n^-	index of refraction
$\hat{n}$	length of a silicate chain
$\bar{n}$	average length of a silicate chain
N_i	ion fraction of i
$N_i(z)$	Neumann Function of order i
p	constant
q_c	heat flux due to conduction
q_{in}	heat flux into surface element of slag
q_{out}	heat flux out of surface element of slag
q_r	heat flux due to radiation
q_t	total heat flux
q^m	heat generation per unit volume per unit time
Q	average heat flux
Q_c	average heat flux due to conduction
r_c	convection heat transfer resistance
r_r	linearized radiation heat transfer resistance
r_t	total heat transfer resistance
r_w	wall heat transfer resistance

R	radius
R_i	inner radius
R_o	outer radius
s	optical thickness
$S(x)$	uncertainty of x
s_λ	monochromatic scattering coefficient
S	mixing parameter
t	time
T	temperature
$\overline{T}$	average temperature of slag element
T_B	bulk temperature of slag bath
T_o	amplitude of periodically varying forcing temperature
T_∞	temperature of the surroundings
$\overline{T}_\infty$	average temperature of the surroundings
V	velocity of sound
W	solid angle
x	sample dimension
X_i	mole fraction of i
$Y_i(z)$	Bessel Function of the second kind of order i
α	absorption coefficient
α_λ	monochromatic absorption coefficient
$\alpha_{\lambda m}$	molar monochromatic absorption coefficient
β	thermal coefficient of expansion
β^*	weighted wavelength distribution
δR	minimum cylindrical sample size

λ	wavelength
ν	kinematic viscosity
ρ	density
σ	Stephen-Boltzman constant
τ	thermal time constant
τ_λ	monochromatic transmission
ϕ	phase angle
ϕ_c	correction phase lag
ϕ_m	measured phase lag
ω	angular frequency
Gr	Grashof number
Pr	Prandtl number

<u>ACKNOWLEDGEMENTS</u>

I. INTRODUCTION

The slag in metallurgical operations may participate to an appreciable extent in the heat transfer processes occurring within the system. Heat transfer in liquid glasses and slags can occur by conduction, convection and radiation. It is the purpose of the investigation reported here to study the combined effects of conduction and radiation heat transfer in glasses similar to metallurgical slags.

Previous studies of combined conduction and radiation heat transfer in diathermanous materials*, have been limited to materials with low absorption coefficients, such as gases, window glass, and tanks of liquid glass containing minor amounts of iron oxide. The results of these investigations indicate that at high temperatures, the dominant mechanism of heat transfer in the bulk material is "radiation conduction". However, for glasses containing large amounts of ferrous ions, the mean free path of photons within the glass may decrease to the extent that radiation conduction no longer is dominant.

In this work, a new periodic steady-state technique has been developed to measure the effective thermal diffusivity of liquid glasses similar to metallurgical slags. Glasses containing 14 to 25 wt. % FeO and having a lime to silica ratio between 1.0 and 1.5 have been studied at temperatures up to 1500°C.

Transmission measurements were also made on glasses containing 0 to 15% FeO to determine the monochromatic absorption coefficients for the

---

* Materials transparent to infrared radiation.

visible and infrared spectra. Using these data, an approximate radiation conductivity was calculated. The relative importance of conduction and radiation to the overall heat transfer process was then determined.

II. LITERATURE SURVEY

While extensive investigation of the heat transfer process in glasses similar in composition to metallurgical slags has not been conducted, there have been many thorough studies of the heat transfer process in glass. This topic can be divided into three basic areas: 1) the general relationships to describe combined conduction and radiation heat transfer in glass, 2) the absorption spectrum of glass, and 3) the heat transfer properties of glass. A brief review of the mathematical analysis of combined conduction and radiation heat transfer is combined with the literature survey. This analysis and the influence of the absorption spectra and heat transfer properties on heat transfer in glass will be considered in more detail when the interpretation of the experimental results are discussed.

II.1 General Relationships

For absorbing and emitting media, the general equation of transfer for combined radiation and conduction[1] in a stagnant glass body is

$$\rho C_p \frac{\partial T}{\partial t} + \nabla \cdot (q_c + q_r) = q^m \qquad (II.1-1)$$

where

$$\nabla \cdot q_c = \nabla \cdot (K_c \nabla T) \qquad (II.1-2)$$

$$\nabla \cdot q_r = \int_{\lambda=0}^{\infty} \alpha_\lambda [4e_{b\lambda}(\lambda,T) - \int_{w=0}^{4\pi} i_\lambda'(\lambda,W)\, dW] d\lambda \qquad (II.1-3)$$

ρ = density, g/cm³

C_p = heat capacity, cal/gm · °K

T = temperature, $^\circ$K

t = time, sec

q^m = heat generation per unit volume per unit time, cal/cm^3 $\cdot$ sec

k_c = thermal conductivity, cal/cm $\cdot$ sec $\cdot$ $^\circ$K

α_λ = monochromatic absorption coefficient, cm^{-1}

$e_{b\lambda}$ (λ, T) = monochromatic black body emissive power, cal/cm^2 $\cdot$ sec $\cdot$ μm

i'_λ (λ, W) = directional monochromatic intensity, cal/cm^2 $\cdot$ sec $\cdot$ μm $\cdot$ sr

At steady state and with no heat generation within the medium, Equation (II.1-1) becomes

$$\nabla \cdot (q_c + q_r) = 0 \qquad\qquad (II.1-4)$$

however, it is still necessary to make several simplifying assumptions to obtain an analytical solution to this equation of transfer.

The concept of diffusion-like transport of radiant energy by absorption and reradiation in glasses was first proposed by Kellett[2]. This investigation of one-dimensional energy transport by radiation and conduction between infinite parallel plates separated by a glass layer led to the formulation of a radiation conductivity and an effective thermal conductivity for grey glasses. A grey glass is a glass that has a constant absorption coefficient, α. Czerny and Genzel[3] and Geffecken[4] generalized the results of Kellett to include the diffuse nature of radiation absorption and reradiation within glass. For combined radiation and

conduction within large bodies of glass, Czerny and Genzel proved the effective thermal conductivity of the heat transfer process, K_{eff}, equaled the thermal conductivity of the glass, K_c, plus the radiation conductivity, K_r,

$$K_{eff} = K_c + K_r \qquad \text{(II.1-5)}$$

The radiation conductivity for a gray glass with absorption coefficient, α, and refractive index, n, equals

$$K_r = \frac{16}{3} \frac{n^2 \sigma T^3}{\alpha} \qquad \text{(II.1-6)}$$

where σ is the Stephen-Boltzman constant, and T is the absolute temperature of the glass.

With this simplification, Equation (II.1-3) becomes

$$\nabla \cdot q_r = \nabla \cdot (K_r \nabla T) \qquad \text{(II.1-7)}$$

and Equation (II.1-4) equals

$$\nabla \cdot (K_c \nabla T + K_r \nabla T) = \nabla \cdot (K_{eff} \nabla T) = 0 \qquad \text{(II.1-8)}$$

Then by integrating Equation (II.1-8), the total heat flux, q_t, equals

$$q_t = -K_{eff} \nabla T \qquad \text{(II.1-9)}$$

A more rigorous treatment of the radiation conductivity by Genzel[5] made it possible to calculate the radiation conductivity of a non-gray glass. To apply this method, the absorption spectra was approximated by a series of steps. Czerny, Genzel and Heilmann[6] developed a graphical technique to determine the radiation conductivity for any glass. For this

case, the radiation conductivity equals

$$K_r = \frac{16}{3} n^2 \sigma T^3 F \tag{II.1-10}$$

where F is the mean free path of a photon within the glass. The value of F is equal to the area under the curve obtained by plotting $1/\alpha_\lambda$ for the glass at the desired temperature versus a specially weighted wavelength scale, $B^*(\frac{\lambda T}{c_2})$. This scale is defined by

$$B^*(\frac{\lambda T}{c_2}) = \frac{\pi}{4\sigma T^3} \int_0^\lambda \frac{e_{b\lambda}(\lambda,T)}{\partial T} \tag{II.1-11}$$

where $e_{b\lambda}(\lambda,T)$ is given by Planck's Law, and c_2 is equal to 1.4387 cm °K.

Values of B^* for $(\frac{\lambda T}{c_2})$ between 0 and infinity are presented in Table II.1-1. These values are used in a later chapter to calculate the radiation conductivity from measured absorption spectra.

For combined radiation and conduction heat transfer in a diathermanous material, the rate at which a transient temperature gradient travels is dependent on the effective thermal diffusivity of the medium[7]. This effect diffusivity is equal to

$$k_{eff} = K_{eff}/\rho c_p \tag{II.1-12}$$

The diffusion approximation and the resulting radiation conductivity may be used to describe heat transfer in glasses only if the radiant energy entering the glass body is absorbed and reradiated many times. This sample size limitation is expressed in terms of the optical thickness, s, of the sample.

$$s = \alpha x \tag{II.1-13}$$

TABLE II.1-1

Values of B* Used to Determine F

$(\lambda T/c_2)$	B*
0	0.00000
0.08	0.004939
0.09	0.01295
0.10	0.02703
0.12	0.07584
0.14	0.1482
0.16	0.2340
0.18	0.3232
0.20	0.4688
0.22	0.4867
0.24	0.5558
0.26	0.6157
0.28	0.6672
0.30	0.7112
0.35	0.7945
0.40	0.8505
0.45	0.8886
0.50	0.9153
0.60	0.9481
0.80	0.9767
1.00	0.9878
1.20	0.9928
∞	1.0000

where x is the sample thickness.

The optical thickness must be greater than about 3 or 4 for the radiation conductivity to apply for planar cases and for cylindrical geometries,

$$\alpha(R_o - R_i) > 7 \qquad \text{(II.1-14)}$$

where R_o and R_i are the outer and inner radius of the cylinder, respectively. For a non-gray glass, the smallest monochromatic absorption coefficient in the wavelength region of significant thermal energy determines the optical thickness of the material[1].

Because of the convenience in describing radiation heat transfer in glass by the radiation conductivity, this concept has been used and misused in many investigations. A review of the relevant literature has been prepared by Gardon[8].

II.2 The Absorption Spectra of Glasses

Several techniques have been developed for measuring the absorption spectra of solid and liquid glasses. Most of the techniques are based on measuring the transmitted fraction, τ_λ, of monochromatic light of wavelength λ, which passes through a sample of thickness x. The absorption coefficient, α_λ, is calculated from Lambert's Law,

$$\tau_\lambda = \exp(-\alpha_\lambda x) \qquad \text{(II.2-1)}$$

Smith[9] has presented a critical review of the techniques used to measure the absorption coefficient for solid samples. For liquids, Genzel[10] has developed a method for placing a platinum mirror in a liquid glass sample. By measuring the transmission for several glass depths, the absorption

coefficient can be found. Grove[11] employed a platinum crucible which had parallel transparent windows to measure the absorption of liquid glasses. The transmission through an empty and full crucible were compared to determine the absorption coefficient.

The only investigation on the absorption of glass containing as much as 4% iron oxide was performed by Coenen[12]. To study the effect of Fe_2O_3 on the absorption of glass, the melts were prepared under oxidizing conditions. The effect of FeO was determined by using a reducing atmosphere. The results of this investigation for the temperature range of 20 to 1400°C indicate that Lambert's Law, Equation (II.2-1), is obeyed by these glasses. However, the absorption of FeO does not obey Bouguer's Law, i.e. the absorption is not linear with respect to concentration of FeO. Changes in the absorption spectra versus temperature were reported, and the radiation conductivities were calculated. This matter will be discussed later. A review of the effect of many oxides on the absorption of glasses is presented by Weyl[13].

II.3 The Heat Transfer Properties of Glass

The important properties of glass which determine the processes of heat transfer are the absorption spectra, the effective thermal conductivity, and the effective thermal diffusivity. Many techniques have been employed for measuring the effective thermal conductivity and diffusivity of glasses. Acloque[14] presents an extensive review of the various steady-state and transient methods for these measurements.

A periodic steady-state technique for measuring the thermal diffusivity of solids was first proposed by Cowan[15]. Methods based on this

idea were developed by Bre[16], Charnock[6], Grove[11], Van Zee[17], and Sevastyahov[18] to determine the effective diffusivity of liquid glasses containing minor amounts of iron oxide. The basic principle of these experiments is to measure the periodically varying temperature at two points within the glass melt. The effective diffusivity can then be calculated from the phase angle between the two temperatures or from the difference in amplitude of the two waves.

Eryou and Glicksman[19] have used a steady-state technique to measure the thermal conductivity of an iron free glass.

In general, the results of these investigations prove that the effective thermal conductivity as derived by Czerny, Genzel and Heilmann[6], Equation (II.1-10), is valid when the optical thickness of the sample is large enough for the diffusion approximation to be applied.

III. OUTLINE AND PLAN OF WORK

The preliminary experimental techniques that were used to measure the effective thermal diffusivity of liquid glass are described in Appendix A. In these experiments, a small glass sample was melted in a furnace which consisted of two metal foil strip heaters. Surface tension held the glass in contact with the heaters and prevented the material from leaving the hot zone. By oscillating the temperature of the heaters in a known manner, and measuring the response of thermocouples at fixed positions within the liquid, the effective thermal diffusivity of the sample could be found. However, after two years of development work, this technique was abandoned because it was not possible to solve the important experimental difficulties.

With the knowledge obtained from these preliminary experiments and the results of the transmission measurements made on glasses containing 0 to 14 wt. % FeO, a new periodic steady-state method for measurement of the thermal diffusivity of liquid glass was developed. Using this technique, the effect of composition (wt. % FeO and lime to silica ratio) on the effective thermal diffusivity of liquid glasses for the temperature range of 1300°C to 1500°C was determined. The results of these experiments and of the transmission measurements should provide sufficient information to determine the relative importance of radiation and conduction to the overall heat transfer process in glasses whose compositions are similar to those of metallurgical slags.

IV.   EXPERIMENTAL APPARATUS AND PROCEDURE

In order to determine the relative importance of radiation and conduction to the overall heat transfer process, the absorption coefficients and the thermal conductivity of the liquid glasses must be determined. To determine the monochromatic absorption coefficients for the visible and infrared spectra, the transmission through solid glass samples was measured. A new periodic steady-state technique was used to measure the effective thermal diffusivity of liquid glasses. The equipment and methods used to perform these measurements are described in this chapter.

IV.1 Transmission Measurements

Transmission measurements were made on quenched samples of glass to determine the monochromatic absorption coefficient for glasses containing up to 15 wt. % FeO. The absorption coefficients for the visible and infrared spectra were calculated using Lambert's Law, Equation (II.2-1). A schematic representation of the measurements is shown in Figure IV.1-1.

The glasses which were used in these experiments were made from reagent grade chemicals which were thoroughly mixed by tumbling for eight hours. The mixture of powders was then fused in an inductively heated Armco-iron crucible at approximately 1400°C. A reducing atmosphere was produced within the crucible by a consumable graphite crucible lid. The approximate temperature of the glass was measured by a Pt/Pt-10% Rh thermocouple which protruded through a hole in the graphite top. To prevent contamination of the glass by the thermocouple protection tube, the
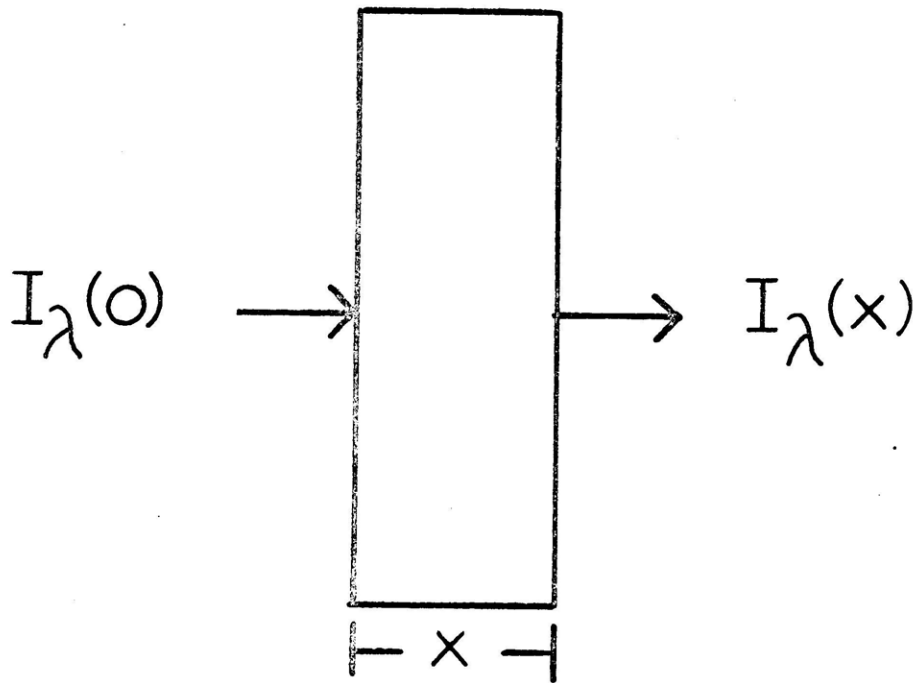
$$\tau_\lambda = \frac{I_\lambda(x)}{I_\lambda(0)} = e^{-\alpha_\lambda x}$$

Figure IV.1-1   A schematic representation of the method for measurement of the monochromatic absorption coefficients.

thermocouple was placed just above but not in the liquid glass.

The samples were obtained by drawing the liquid glass into copper tubes of rectangular cross-section. To free the glass, the copper was dissolved in nitric acid. Then the samples were cut, mounted and polished to obtain rectangular samples approximately 0.4 mm thick, 6.0 mm wide, and 20 mm long, with parallel optically polished surfaces. The measurements for 0.3 μm to 2.1 μm were performed on a Gary recording spectrophotometer. For 2.5 μm to 10.0 μm, a Beckman IR-12 recording spectrophotometer was used.

IV.2 Measurement of the Effective Thermal Diffusivity

A periodic steady-state technique was used to measure the effective thermal diffusivity of optically thick liquid glass samples which contained large amounts of FeO. For these experiments, a periodically varying temperature was produced at the inner surface of the glass sample by heating a molybdenum wire with a periodically varying current. The temperature at the outer surface was measured by a Pt-30% Rh/Pt-6% Rh thermocouple which was contained in a small alumina protection tube. The effective thermal diffusivity of the glass was determined from the difference in phase between the two periodically varying temperatures.

The hollow cylindrical glass sample of inner radius, R_i, and outer radius, R_o, was held in an Armco-iron crucible. The molybdenum wire (radius equal to 0.19 mm) was positioned axially within the sample and was insulated from the glass and crucible by a small alumina tube (inner radius equal to 0.20 mm; and outer radius, R_i, equal to 0.41 mm), see Figure IV.2-1. Heavier molybdenum wires were used to make the external
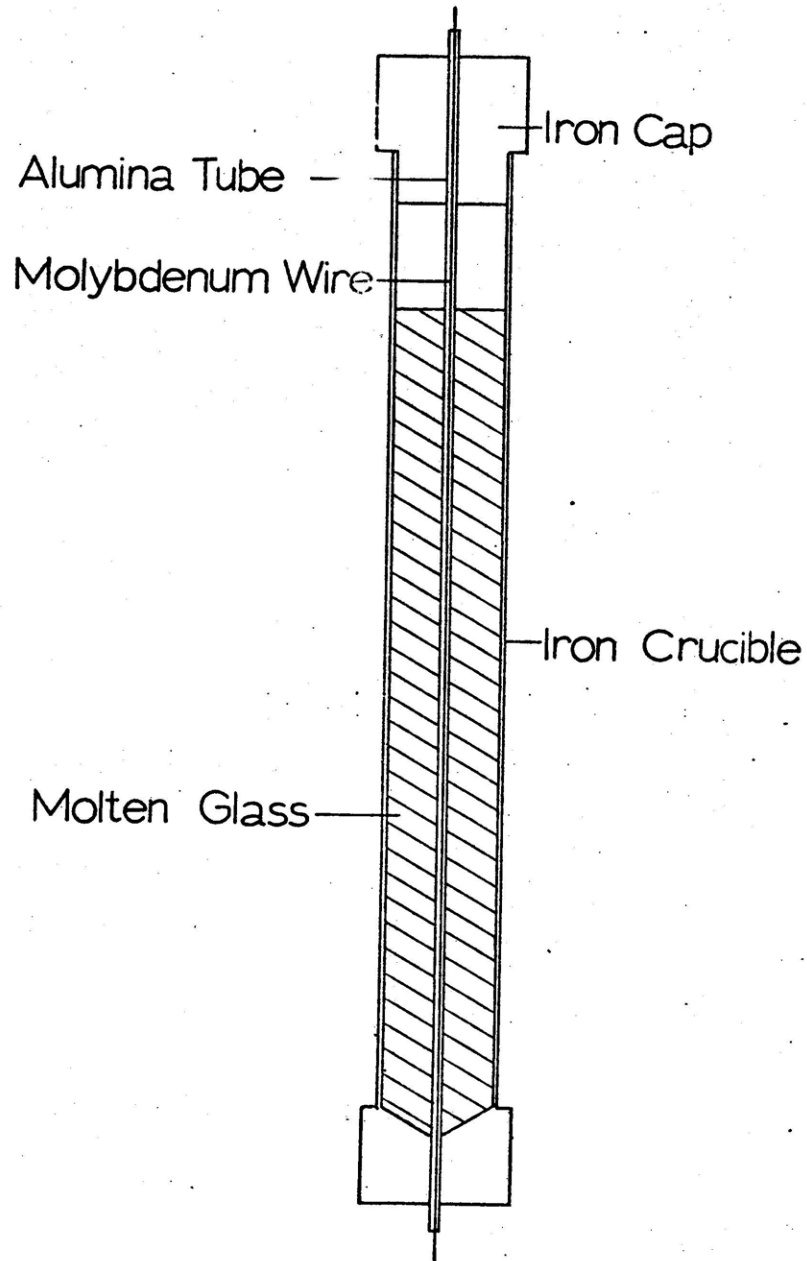
Figure IV.2-1 Glass sample and container for thermal diffusivity measurements.

connections to the thin molybdenum wire within the crucible. The heavier wires were also insulated by alumina tubes.

To provide a protective atmosphere for the assembly, it was placed in a large alumina crucible which was continuously flushed with purified argon. Uniform temperatures up to 1500°C were attained by placing the assembly in a platinum-wound furnace, see Figure IV.2-2. A hole through the furnace and large alumina tube allowed the thermocouple to be placed in contact with the iron crucible wall. To prevent air from leaking into the apparatus around the thermocouple protection tube, a positive pressure was maintained within the assembly. The gas system used to produce the purified argon is shown in Figure IV.2-3.

The glass samples used in this experiment were prepared in a manner similar to that used for determination of the absorption coefficients. The liquid oxide was drawn into a long round fused silica tube (inner radius approximately equal to R_0 minus 0.25 mm) to obtain a cylindrical specimen. To remove the specimen, the tube wall was gently cracked and peeled away to expose the glass. A longitudinal notch was machined along the rod to receive the molybdenum wire and alumina tube.

The rate at which the periodically varying temperature, produced at the inner surface of the sample, progresses through the glass is a function of the effective thermal diffusivity of the glass. The rate will be represented by the phase lag between the current in the wire within the sample and the temperature measured at the outer surface of the iron crucible. The relationship between the phase angle, ϕ, and the thermal diffusivity is developed in Appendix B.
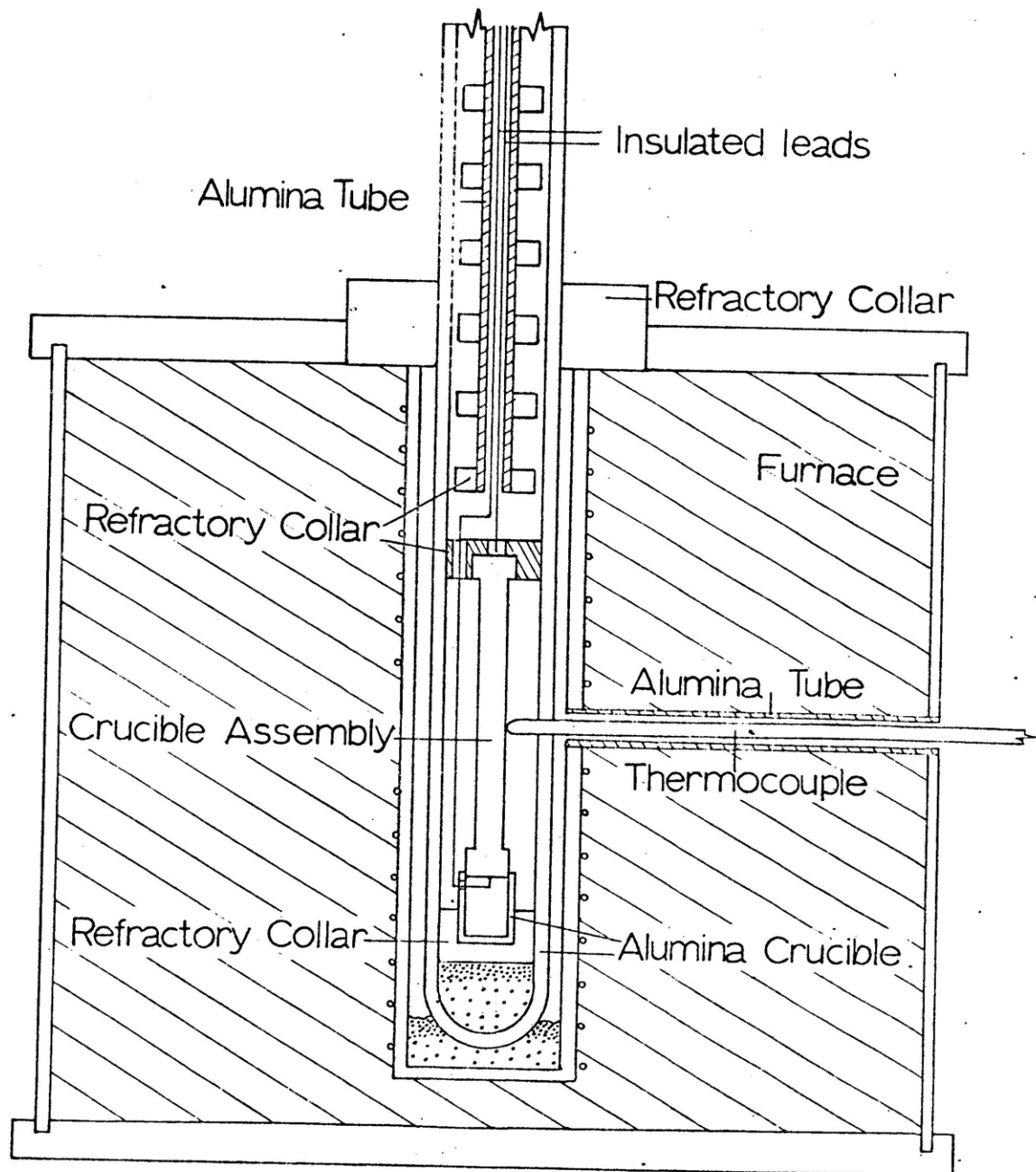
Figure IV.2-2 Experimental apparatus for measuring the thermal diffusivity of liquid glasses.
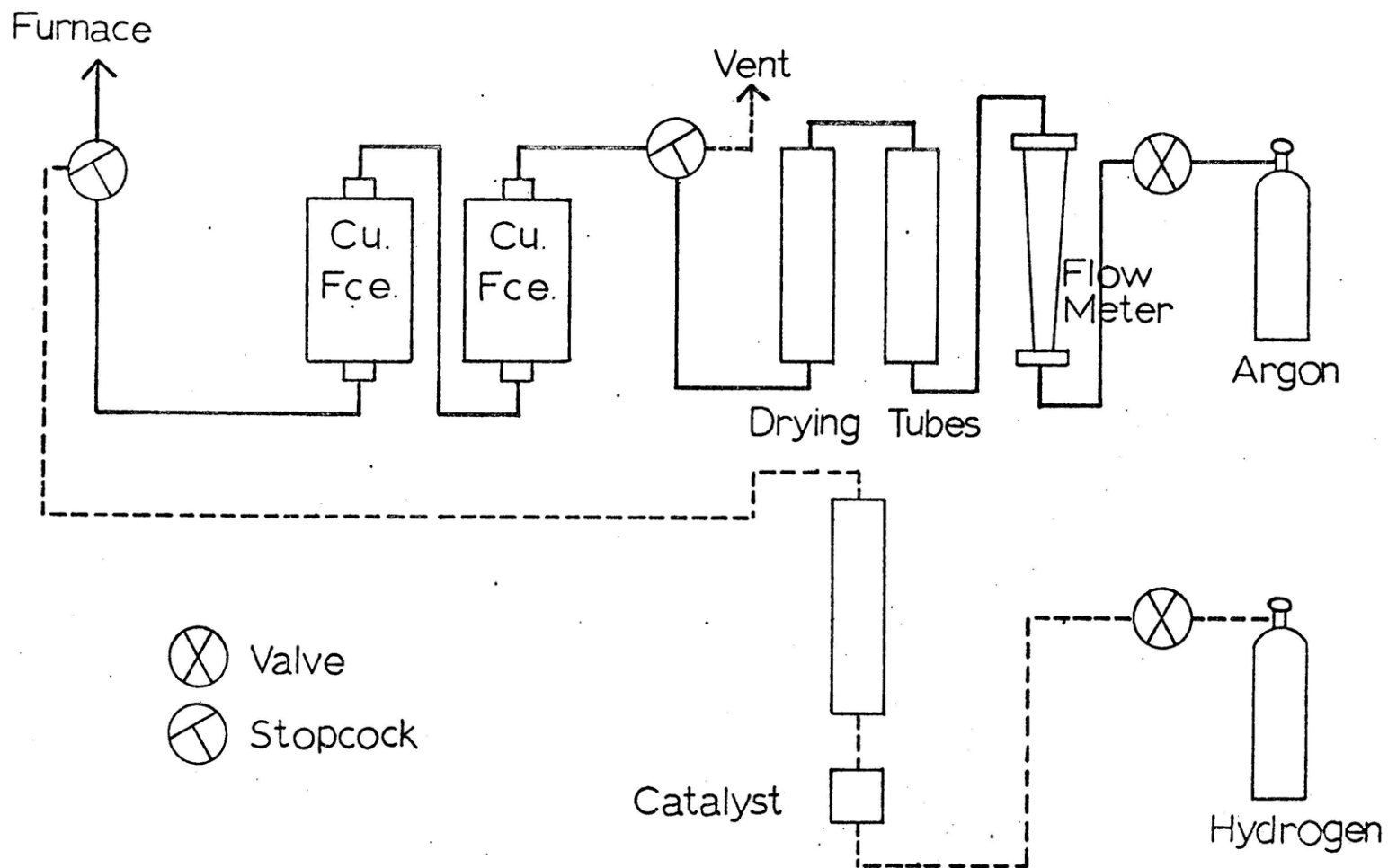
Figure IV.2-3   The flow chart of the gas system used to provide a protective
atmosphere for the apparatus used to make the thermal diffusivity measurements.

The periodically varying heating current was produced by a Wenking potentiostat which was driven by a Wavetech function generator. The thermocouple output was recorded on a Dupont DTA-900 recorder. To measure the phase angle, "tic" marks were added to the thermocouple output. The tic marks were produced by a Techtronics pulse generator and coincided with the nodes of the periodic current. The approximate temperature response and thermocouple response for a square-wave heating current are shown in Figure IV.2-4.

After assembling and bringing the apparatus up to a steady-state temperature, experiments may be performed using periodically varying currents of several different frequencies. Also, experiments may be performed at one or more steady-state temperatures.

To determine the phase lag resulting from the small alumina tube around the molybdenum wire and the characteristics of the measuring apparatus, experiments were performed using the apparatus described in Appendix A. This phase angle is subtracted from the measured phase lag to determine the phase lag of the glass only.
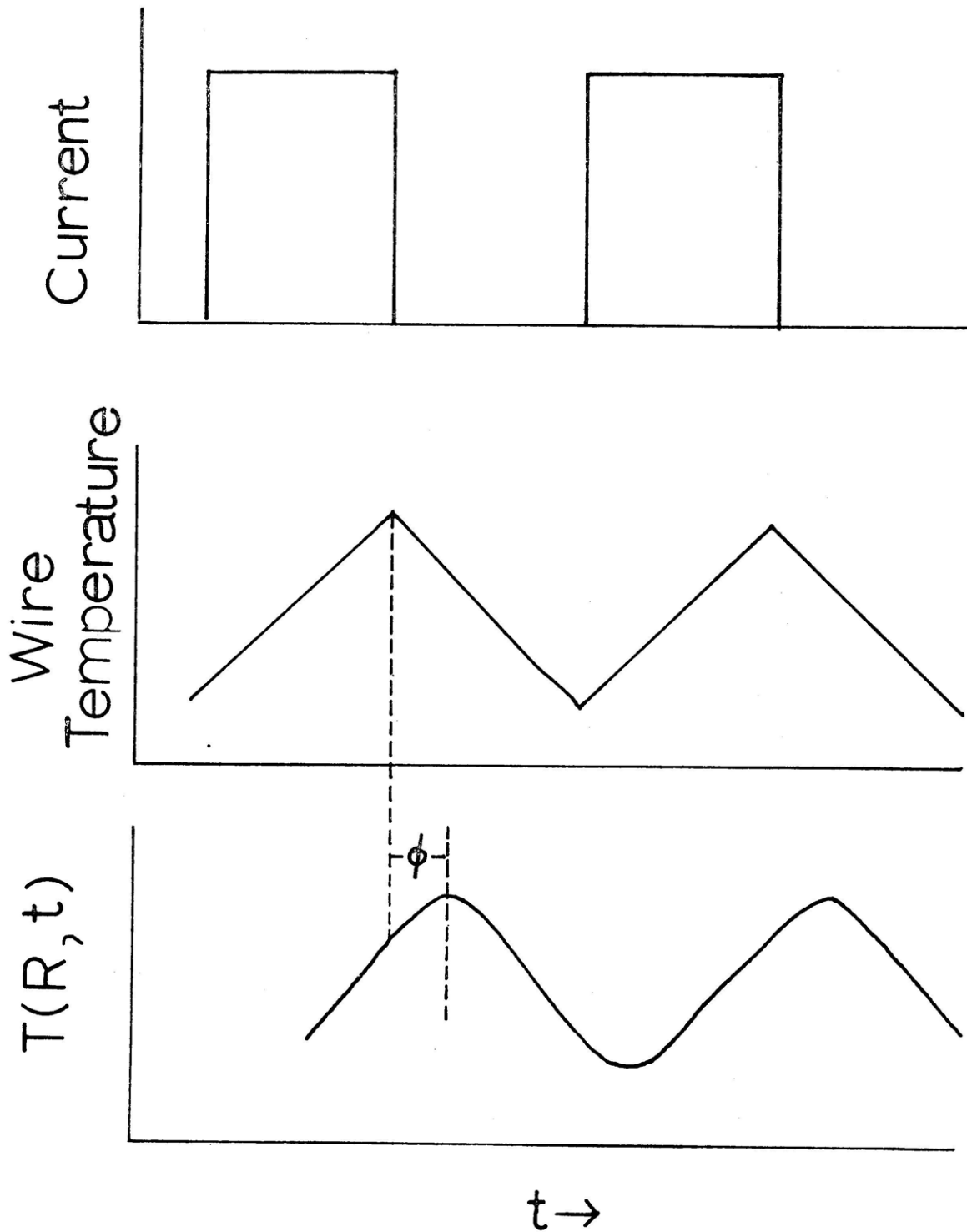
Figure IV.2-4   Representation of method for measuring the Phase
Angle, ¢, for a square-wave heating current.

V. EXPERIMENTAL RESULTS

At elevated temperatures, heat transfer through diathermanous mate-
rials occurs by conduction and radiation. In the investigation reported
here, an experimental program was undertaken to determine the relative
importance of each process, and the overall rate of heat transfer in
glasses similar in composition to metallurgical slags. In this chapter,
the results of this program are presented.

V.1 Transmission Measurements

The properties of diathermanous materials that determine the rate of
thermal radiation heat transfer within the material are the monochromatic
absorption coefficients for the visible and infrared spectra. Transmission
measurements were performed on thin solid glass samples to determine the
absorption spectra for glasses containing up to 14.2% (#3a) FeO, see
Table V.1-1. Using these data, the radiation conductivities and minimum
dimension of optically thick samples were calculated.

As an example of the type of data obtained from the transmission
experiments, the results for an experiment performed on glass containing
14.2% FeO (#3a) are shown in Figures V.1-1 and V.1-2. The discontinuity
at 1.5 μm in Figure V.1-1 was the result of changing the limits of the
ordinate scale at that wavelength. Using the data obtained from the
transmission experiments, the absorption spectra for these glasses were
calculated using Lambert's Law,

TABLE V.1-1

Composition of Glass for Transmission Experiments

Glass Number	Weight Percentage				
	FeO	CaO	SiO$_2$	Al$_2$O$_3$	MgO
1	0.0	36.6	36.6	14.6	12.2
2	7.1 (6.27)[+]	34.0	34.0	13.5	11.4
3a	14.2 (12.6)	31.4	31.4	12.5	10.5
6	14.2	39.8	26.6	10.6	8.8
7	20.0 (20.7)	37.1 (25.9)*	24.8 (22.7)	9.9 (8.7)	8.2 (7.33)

[+] Compositions listed in parentheses have been determined by chemical analysis.

* The chemical analyses for lime are wrong.
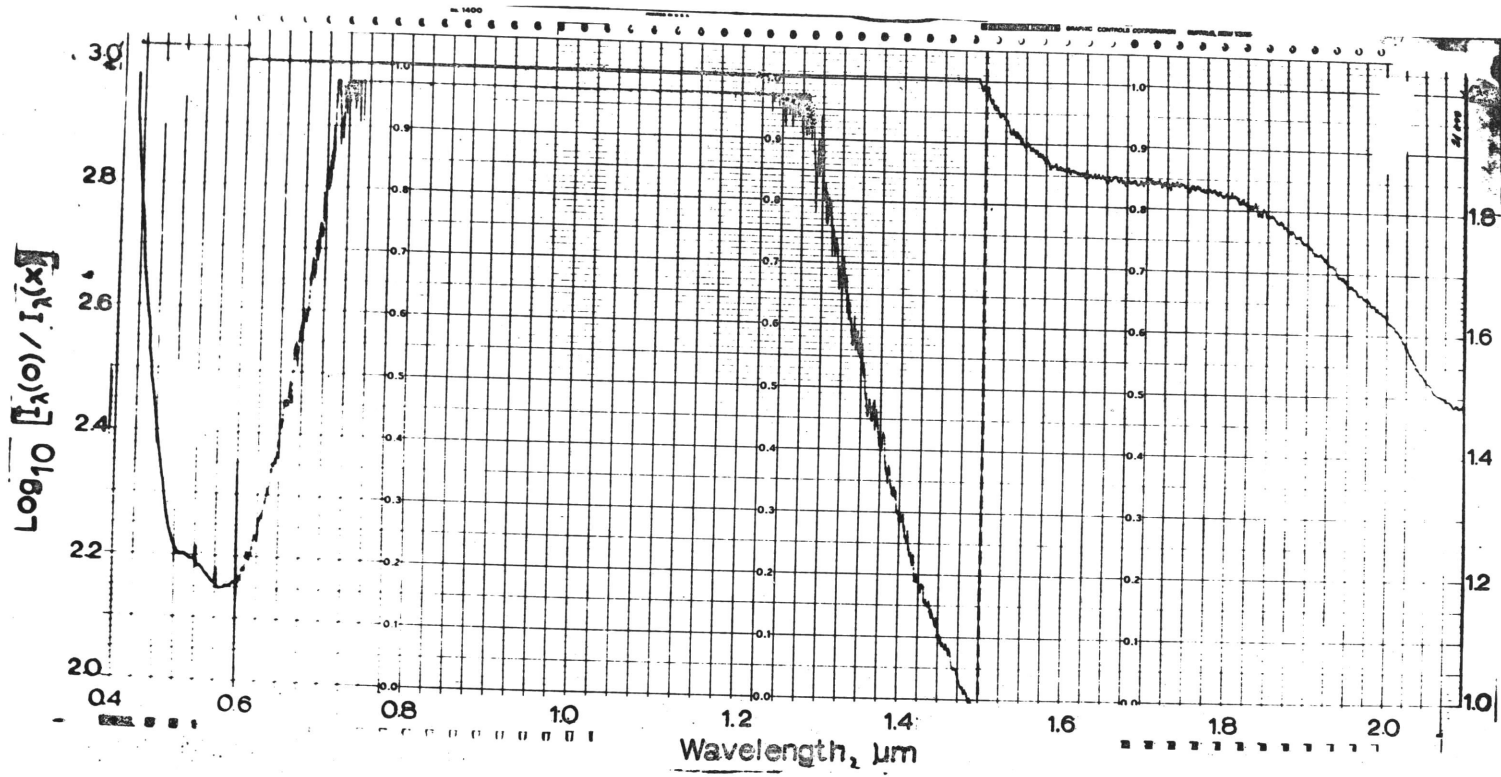
Figure V.1-1   Transmission experiment results for glass containing 14.2% FeO (#3a) for the wavelength interval between 0.4 μm and 2.1 μm.
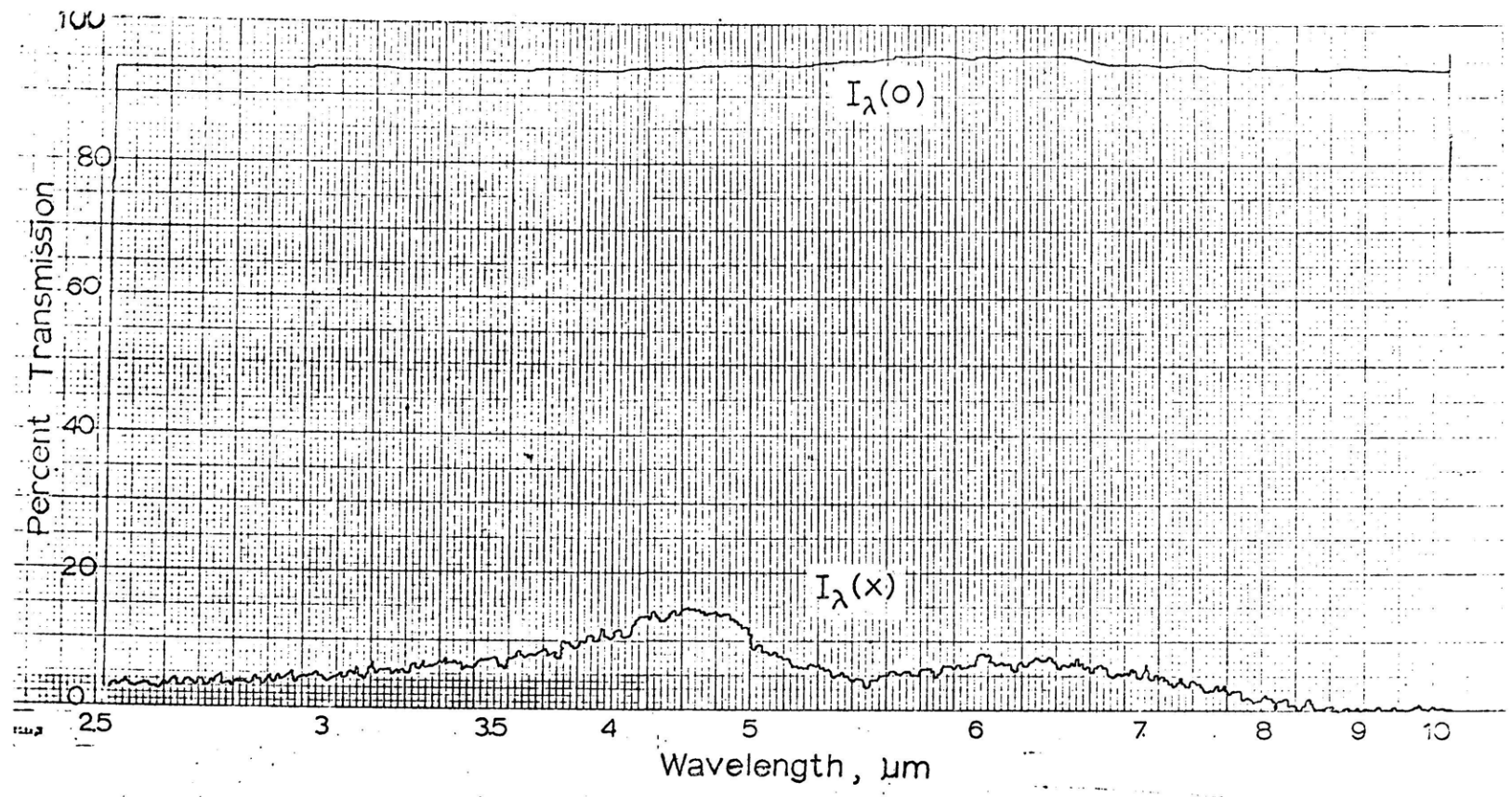
Figure V.1-2   Transmission experiment   results for glass containing 14.2% FeO
(#3a) for the wavelength interval between 2.5 μm and 10.0 μm.

$$\tau_\lambda = \frac{I_\lambda(x)}{I_\lambda(o)} = e^{-\alpha_\lambda x} \qquad (II.2-1)$$

The absorption coefficients determined from these calculations are shown

in Figure V.1-3. The radiation conductivity,

$$K_r = \frac{16}{3} n^2 \sigma F T^3 \qquad (II.1-10)$$

and the minimum dimension of an optically thick sample,

$$R_o - R_i = 7/\alpha \qquad (II.1-14)$$

were also calculated for glasses 1, 2 and 3a, and these results are

presented in Table V.1-2.

Experiments performed to make samples of glasses with higher lime to

silica ratios, glasses #6 and 7, were not successful. The compositions

of these oxide melts were apparently outside of the glass-forming range,

and only crystalline samples could be made. For crystalline materials, the

grain boundaries produce scattering and the resulting measurements would

determine the extinction coefficient,

$$E_\lambda = \alpha_\lambda + s_\lambda$$

where s_λ is the monochromatic scattering coefficient. These measurements

were not pertinent to the investigation and, therefore, were not pursued

further.

V.2 Thermal Diffusivity Measurements

The rate at which a transient temperature gradient travels in a

diathermanous material is determined by the effective thermal diffusivity
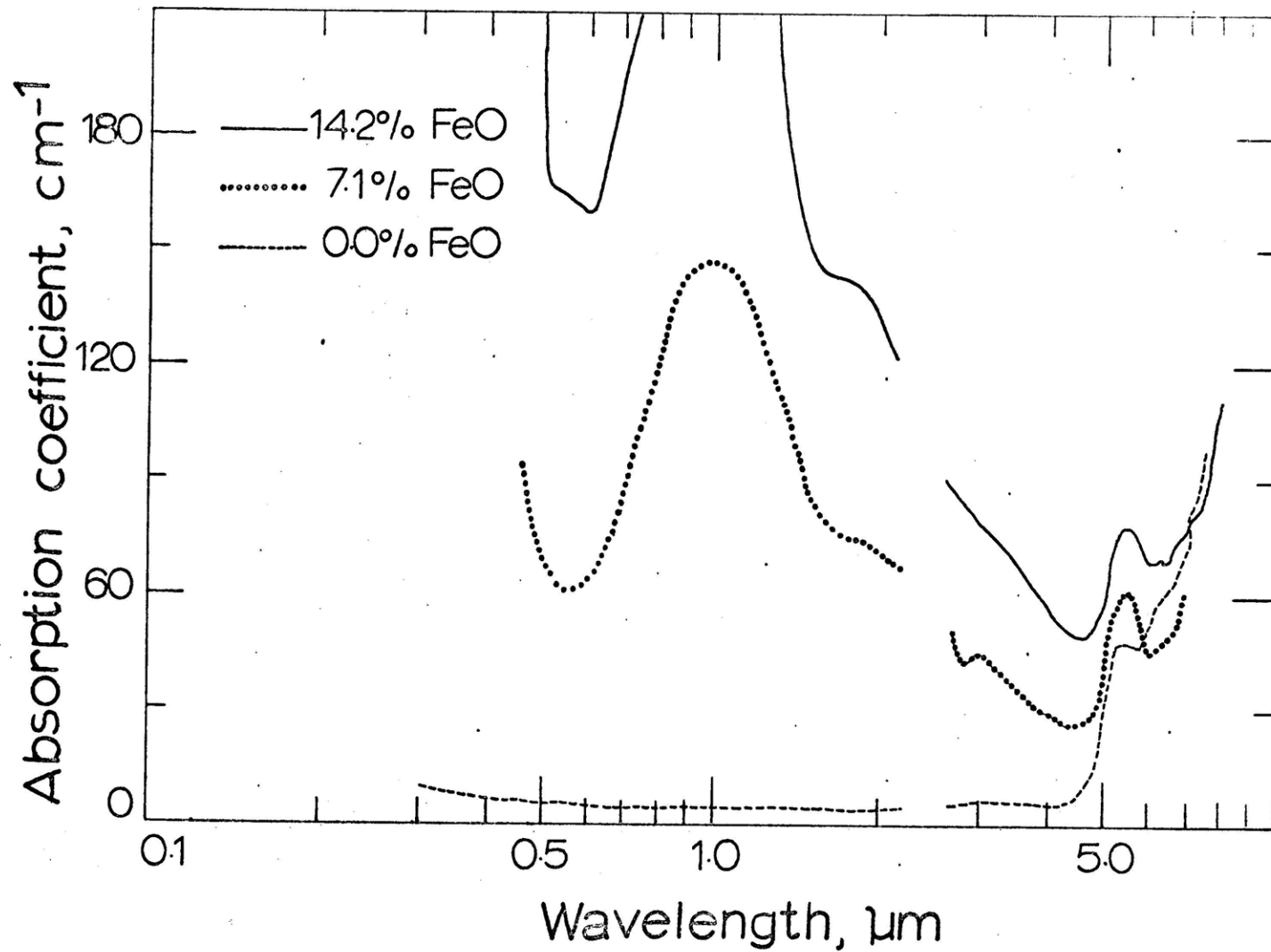
Figure V.1-3   Monochromatic absorption coefficients for glasses containing 0.0%
(#1), 7.1% (#2), and 14.2% (#3a) FeO.

of the material. Using the apparatus described in Section IV.2, phase shift measurements were made on liquid glasses which contained up to 25 wt. % FeO to determine their effective thermal diffusivities. The results of the experiments are reported in two sections; the results of the calibration experiments, and the results of the experiments performed on liquid glasses.

V.2.1 Calibration Experiments

The analysis of the experimental apparatus presented in Appendix B proves that the phase lag for all of the components of the apparatus is equal to the sum of the individual phase lags. Consequently, the phase angles for the components of the experimental apparatus excluding the liquid glass must be determined, so that the phase lag of the glass can be calculated from the measured phase angles. The effective thermal diffusivity of the liquid glass is then obtained from the phase angle of the glass only.

The phase lag associated with the components of the experimental apparatus were determined using the apparatus described in Appendix A. This technique was employed because it was possible to place the thermocouple in firm contact with one of the strip heaters of this furnace, whose temperature could then be sinusoidally oscillated around any desired steady-state value. With this apparatus, it was not possible to measure the phase lag of the small alumina tube, see Figure IV.2-1. This angle was determined by using the computer program described in Appendix B.2, for the properties[20] and dimensions of the tube. The total correction phase lag, ϕ_c, was found by adding the two results. The data for these experiments are

TABLE V.1-2

Values of K_r and δR at 1300°C

Glass Number	K_r X 10^3 (cal/sec·cm·°K)	δR (cm)
1	6.3	1.7
2	1.0	0.28
3a	0.7	0.13

shown in the first four columns of Table V.2-1.

To check the results of these experiments, the phase angles associated with the characteristics of the electronic equipment, the alumina tube and the thermocouple protection tube were individually determined, and added to obtain the correction phase lag. The results of these experiments are in good agreement with the measured correction phase lag and are shown in the fifth column of Table V.2-1.

V.2.2 Effective Thermal Diffusivity Measurements

The periodic steady-state technique described in Section IV.2 was used to measure the effective thermal diffusivity of liquid glasses similar in composition to metallurgical slags. These experiments were performed on glasses which contained 14.2%, 20% and 25% FeO and had a lime to silica ratio of 1.0 and 1.5, see Table V.2-2.

For each experiment, at least ten cycles were measured and the average value and standard deviation calculated. To determine the phase lag of the glass only, the measured correction phase lag was subtracted from the average value of the total phase lag. The effective thermal diffusivity of the glass sample was then found from the results of the analysis presented in Appendix B. The average value and standard deviation of the effective thermal diffusivity experiments are tabulated in Table V.2-3.

TABLE V.2-1

Results of Calibration Experiments

Frequency (Hz)	Phase Lag (Degrees)			
	$\phi_{apparatus}$	ϕ_{tube}	$\phi_{c,measured}$	$\phi_{c,calculated}$
0.01	1.3	0.00	1.3	1.2
0.03	6.0	0.01	6.0	4.0
0.05	8.4	0.05	8.5	5.8

TABLE V.2-2

Composition of Glass for Effective
Thermal Diffusivity Experiments

Glass Number	Weight Percentage				
	FeO	CaO	SiO$_2$	Al$_2$O$_3$	MgO
3b	14.2 (12.4)[+]	31.4 (25.9)*	31.4 (33.2)	12.5 (11.3)	10.5 (10.8)
3c	14.2 (11.9)	31.4 (27.5)*	31.4 (32.4)	12.5 (10.4)	10.5 (10.6)
4	20.0 (18.0)	29.3 (23.4)*	29.3 (30.7)	11.7 (10.0)	9.7 (9.47)
5	25.0 (20.6)	27.5 (21.9)*	27.5 (28.5)	10.9 (9.27)	9.1 (8.20)
6	14.2	39.8	26.6	10.6	8.8
7	20.0 (20.7)	37.1 (25.9)*	24.8 (22.7)	9.9 (8.7)	8.2 (7.23)

[+] Compositions listed in parentheses have been determined by chemical analysis.

* The chemical analyses for lime are wrong.

TABLE V.2-3

Results of Effective Thermal Diffusivity Experiments

Glass Number	wt. % FeO	Temperature (°K)	k_{eff} X 10^3 ($\frac{cm^2}{sec}$)
3b	14.2 (12.4)*	1586	3.8 ± 0.7**
		1577	4.0 ± 0.4
		1577	3.6 ± 0.2
		1628	3.9 ± 0.4
		1628	3.8 ± 0.2
		1678	4.8 ± 0.2
		1678	4.5 ± 0.4
3c[††]	14.2 (11.9)	1573	4.1 ± 0.2
		1713	4.6 ± 0.4
		1713	4.8 ± 0.2
		1718	4.5 ± 0.2
		1718	4.9 ± 0.2
4	20.0 (18.0)	1573	3.5 ± 0.4
		1643	3.5 ± 0.2
5	25.0 (20.6)	1567	2.4 ± 0.3
		1567	2.0 ± 0.1
		1644	3.0 ± 0.4
		1644	2.6 ± 0.1
6	14.2	1653	3.4[†]
7	20.0 (20.7)	1603	2.6[†]

* Compositions listed in parentheses were determined by chemical analysis.

** This result was obtained using a pyrometer instead of a thermocouple, see Discussion.

[†] It was not possible to measure enough cycles on glasses of this composition to determine error limits.

[††] Experiments on this glass were performed using large crucibles, δR = 3.7 mm.

VI. DISCUSSION OF RESULTS

Two types of results were presented in the previous chapter: The absorption spectra of solid glass samples containing up to 14.2 wt. % FeO, and the effective thermal diffusivities of liquid glasses which contained up to 25 wt. % FeO. In this chapter, the errors associated with the two experimental procedures and the accuracy of the results are discussed. The effects of temperature and composition on the thermal conductivity and radiation conductivity of glasses are determined from theoretical treatments and data in the literature. Finally, a correlation is developed so that the data obtained from the experiments may be extrapolated to other glass compositions and temperatures.

VI.1 Evaluation of Experimental Measurements

The errors associated with the experimental techniques used to determine the radiation conductivities and effective thermal diffusivities of glasses similar in composition to metallurgical slags are discussed in this section. In the first part of the section, the effects of reflection at the glass-air interfaces and the effect of the temperature on the radiation conductivity are determined. The possible errors in the effective thermal diffusivity experiments due to measuring inaccuracy, convection and not maintaining an optically thick glass sample are discussed in the latter half of this section.

VI.1.1 Radiation Conductivity

To determine accurately the radiation conductivity of a glass at a desired temperature, the absorption spectrum of the glass should be

measured at that temperature. The energy losses due to reflection at the glass-air interfaces must also be determined for the experimental configuration. In the investigation reported here, it was not possible to perform these measurements. As a result, corrections must be applied to the measured absorption spectra. These corrections and the magnitude of the errors in the results are reported.

Because a suitable experimental technique was not available for measuring the absorption of liquid glasses that contained large amounts of FeO, measurements were only made at room temperature. With this information, an approximate radiation conductivity was found by determining the area under the curve produced by plotting $1/\alpha_\lambda$ versus the wavelength distribution, corresponding to the values of β^* listed in Table II.1-1, and temperature equal to 1300°C. The radiation conductivity was then calculated from the area, F, by the relationship

$$K_r = \frac{16}{3} n^2 \sigma F T^3 \qquad (II.1-10)$$

Previous investigations of glass containing up to 1% FeO indicate that the absorption spectrum of FeO is lower at 1300°C to 1400°C than at 20°C. However, the exact percentage decrease seems to be a function of the concentration of FeO as well as the wavelength. Grove and Jellyman[21] have reported that for a glass containing 0.16% Fe_2O_3, melted under reducing conditions, the difference in the absorption spectra is less than 10% for wavelengths between 0.8 μm and 2.6 μm. For glass containing 1% FeO, Coenen[12] indicates a decrease of as much as 60% for the same wavelength band. The results presented by Coenen, however, are of questionable value.

For these experiments, the percentage of total iron in the melts was determined, not the precentage of FeO. Small changes in the ratio of ferrous to ferric ions as the temperature increased could therefore produce the large variations of absorption.[22,23] Generally, the absorption spectra of glasses do not change more than about 10% over wide temperature ranges[24]. Consequently, a 10% decrease in the measured absorption spectra, as suggested by Grove and Jellyman, is assumed to occur as the glass is heated to 1300°C.

The effect of reflection at the glass-air interfaces will also produce a larger value of the measured absorption coefficient. The error for this effect can be determined from the analysis presented by Smith[9]. For a glass with an index of refraction equal to 1.5, the measured absorption coefficients were a maximum of 4% too high. The average error was 2%.

Another uncertainty in the measured absorption spectra was produced by the noise in the recording spectrophotometer output. This error was approximately ±0.5%.

The values of the absorption coefficients were corrected for the errors produced by increasing temperature and reflection. The corrected values of the radiation conductivities and minimum dimension of an optically thick sample were determined and found to be 10% and 12% larger, respectively.

VI.1.2 Effective Thermal Diffusivity

The uncertainty in the results of the phase shift measurements used to determine the effective thermal diffusivity of liquid glasses, can be grouped into three categories: measuring errors, errors produced by

convection in the melt, and the error resulting from using a sample that is not optically thick. These errors are discussed and the magnitude of the uncertainty in the results are determined.

VI.1.2.A Measurement Error

The accuracy of the experimental measurements can be related to the uncertainty of the experimental parameters by the relationship proposed by Beers[25]. For the effective thermal diffusivity, where

$$k_{eff} = F(\phi_m, \phi_c, \delta R) \qquad (VI.1-1)$$

the uncertainty of the value of k_{eff}, $S(k_{eff})$, equals

$$S(k_{eff}) = \pm \quad [(\frac{\partial k_{eff}}{\partial \phi_m})^2 \, S(\phi_m)^2 + (\frac{\partial k_{eff}}{\partial \phi_c})^2 \, S(\phi_c)^2 + (\frac{\partial k_{eff}}{\partial \delta R})^2 \, S(\delta R)^2]^{1/2}$$

$$(VI.1-2)$$

where $S(\phi_m)$, $S(\phi_c)$, and $S(\delta R)$ are the uncertainties of the measured phase lag, correction phase lag, and the position of the alumina tube within the glass, respectively.

The value of $S(\delta R)$ was determined by sectioning samples and measuring the average deviation from the theoretical inner radius, R_i = 0.4 mm. This error resulted from slightly warped tubes, and because the alumina tubes were dissolved by the glass. The rate of attack increased with temperature, percent FeO and lime to silica ratio. However, the error produced by dissolution of the tube could not be greater than 0.2 mm, the tube wall thickness. In practice, the combined error was never greater than 0.2 mm.

The values of $S(\phi_m)$ and $S(\phi_c)$ were equal to the measuring error times 360 degrees divided by the average length of a cycle. The values of the

uncertainties and the partial derivatives, which were determined from the computer results, are shown in Table VI.1-1. By substituting these values into Equation VI.1-2, the values of the uncertainty in the measured effective thermal diffusivities, $S(k_{eff})$, shown in the last row of Table VI.1-1 were calculated. The values of $S(k_{eff})$ were in all cases smaller than or equal to the standard deviation of the experimental results. Therefore, the standard deviation should be used for the uncertainty in the values of the effective diffusivities.

VI.1.2.B Convection

Experimental determination of the thermal conductivity or diffusivity of liquids are very difficult to perform because convection within the melt can produce very large errors. To eliminate this possible error, great care was used in the design and construction of the experimental apparatus. The temperature of the liquid glass must be maintained as nearly constant as is possible to prevent convection.

In an earlier investigation[26], which incorporated a similar but much larger apparatus, the temperature of the outer wall of the crucible was oscillated, and the temperature at the axis of the cylinder measured. When convective stirring occurred in this apparatus, the temperature response became very distorted. A similar response would be expected in the apparatus presently being used when convective stirring was produced. Another criterion for the onset of convection is that the product of the Grashof Number, Gr, times the Prandtl Number, Pr, be greater than 800.[27]

$$Gr \cdot Pr > 800 \qquad\qquad (VI.1-3)$$

where

TABLE VI.1-1

Estimated Values of the Uncertainties of the
Experimental Parameters and of Their Effect on k_{eff}

Parameter	Frequency (Hz)		
	0.01	0.03	0.05
$S(\phi_m)$	0.5°	1.0°	2.0°
$\partial k_{eff}/\partial(\phi_m)$	1.8×10^{-4}	7.2×10^{-5}	5.4×10^{-5}
$S(\phi_c)$	0.5°	1.0°	1.0°
$\partial k_{eff}/\partial(\phi_c)$	1.8×10^{-4}	7.2×10^{-5}	5.4×10^{-5}
$S(\delta R)$	0.2 mm	0.2 mm	0.2 mm
$\partial k_{eff}/\partial(\delta R)$	9.2×10^{-4}	9.1×10^{-4}	9.0×10^{-4}
$S(k_{eff})$	2.2×10^{-4}	2.0×10^{-4}	2.2×10^{-4}

$$Gr \cdot Pr = g\beta(\delta R)^3 \, \Delta T / \nu k_{eff} \qquad\qquad (VI.1-4)$$

Unfortunately, many of these quantities have not been measured for the slags being investigated here, so only approximate values can be used to calculate the maximum value of Gr · Pr. The values of B and ΔT were estimated as 10^{-4} (1/°C) and 5°C, respectively. The values of ν and k were estimated to equal 1 cm²/sec and 0.003 cm²/sec, respectively[26]. For these values and for the larger crucible, δR = 0.37 cm, Gr · Pr was approximately equal to 10. Because this product was much less than 800, and because no distortion was observed in the thermocouple response for any experiment, there must be no convection in the liquid glasses being investigated.

VI.1.2.C Optical Thickness of the Sample

The analysis presented in Appendix B was based upon the diffusion approximation for radiative transport in the liquid glass sample. This approximation is only valid, if the sample being investigated is optically thick. If this condition is not met, serious errors in the measured effective thermal diffusivities can arise[8].

Due to the uncertainty in the calculated values of the minimum dimension of an optically sample previously discussed, another method for checking the validity of this assumption was employed. For measurements performed on a glass sample that is not optically thick, the measured conductivity does not equal the effective conductivity of the glass. In this case, the conductivity is a function of the boundary conditions as well as the material properties, see Equation II.1-3, and not an intensive

property of the material. Consequently, experiments were performed on two different crucible sizes to determine the validity of the assumption. The results of the experiments on the larger glass samples were in good agreement with the results and correlation for the smaller glass samples, see Figure VI.2-2. Therefore, the measured diffusivities are not dependent on the size of the crucibles, and are equal to the effective thermal diffusivities of the glasses investigated.

The experiments on two different sample sizes were performed on the glasses with the lowest concentrations of FeO only. Because the minimum dimension of an optically thick sample decreases with increasing percent FeO, see Table V.1-2, it is concluded that the glasses which contained more FeO are also optically thick.

VI.2 Interpretation of Results

The range of glass compositions and temperatures that could be studied in the investigation reported here were extremely limited by the liquidus temperature of the glasses, recrystallization of the more basic glasses, and the melting point of iron. Based upon theoretical treatments and data available in the literature, the dependence of the thermal conductivity and radiation conductivity on the composition and temperature of the glass are determined. These results are used to derive a correlation between the effective thermal diffusivity and the composition and temperature of the glasses investigated. Using the correlation, it is possible to determine the effective diffusivity of glasses at other temperatures and compositions.

VI.2.1 Thermal Conductivity

Energy transport in dielectric materials can occur by lattice

vibrations, that is by phonon transport, as well as the absorption and re-radiation of quanta of energy, photons. In this section, the effect of temperature and composition on the phonon conductivity, i.e. thermal conductivity, of glass is discussed. A possible correlation between the phonon conductivity and density is also presented. The validity of this correlation for high temperature conductivities is analyzed.

As shown by Kingery[28], the thermal conductivity of glass can be related to the mean free path, L, of a phonon within the glass by analogy to the kinetic theory of gases. The result of this analysis shows that the thermal conductivity is equal to

$$K_c = \frac{1}{3} C_p \cdot V \cdot L \qquad\qquad (VI.2-1)$$

where C_p is the heat capacity per unit volume and V is the average velocity of sound within the glass. As a result, the dependence of the thermal conductivity on temperature and composition can be determined if the dependence of C, V and L on temperature and composition are known.

Kittel[29] has suggested that the mean free path of a phonon within a solid glass sample is of the same order of magnitude as the average length of a structural unit of the material. Since, for a solid, this length is not dependent on temperature; the value of L is not a function of temperature.

Experimentally, it has been shown that the thermal conductivity is a function of the heat capacity only[30,31]. Consequently, the velocity of sound must also be independent of temperature.

Because the viscosity is a colligative property of liquid glass, the

change in the average length of a structural unit of the liquid glass can be inferred from the change in viscosity with temperature. Since the viscosity decreases with increasing temperature[32], the value of L must be decreasing. Eryou and Glicksman[19] have found for liquid water white glass, the thermal conductivity remains constant. Consequently, there must be a compensating increase in the heat capacity and/or velocity of sound in this type of glass which counter balances the decreasing value of L. Charnock[7] has also shown that a constant value of the thermal conductivity is consistent with the results of his investigation. Therefore, since there is no evidence in the literature which indicates the thermal conductivity of any glass changes with temperature, and since there is evidence that at least two glasses have constant thermal conductivities, the thermal conductivity of the glasses studied in this investigation are assumed to be equal to a constant.

The dependence of the phonon conduction on the composition of the glass could be determined if the relationships between the composition of the melt and the heat capacity, velocity of sound, and structure were known. As previously noted, these properties have not been determined for any glasses at high temperature. Using several assumptions and theoretical treatments, it is at least possible to qualitatively determine the dependance of K_c on composition. A theoretical model for predicting the distribution of silicate chain lengths in a binary silicate melt has been developed by Masson[33]. This analysis shows that lime has a much larger effect on the silicate chain than any of the other oxides studied. As a result, it is assumed that the average silicate chain length is a function

of the lime to silica ratio, B, only. Using the results of Masson's model, see Figure VI.2-1, the average length, $\bar{n}$, of the silicate chains of the type $Si_nO_{(2\hat{n}+1)}^{(3\hat{n}+1)-}$ were calculated for lime to silica ratios between 1.0 and 2.33. The average length, $\bar{n}$, was defined by the relationship

$$\bar{n} = \sum_i \hat{n}_i N_i / \sum_i N_i \qquad\qquad \text{(VI.2-2)}$$

where N_i was equal to the ion fraction of species i. The value of $\bar{n}$ is an indication of the average unit size of the silicate structure and should be directly proportional to L, the mean free path of a phonon.

The heat capacity of the oxide mixture, C_p, was calculated from the heat capacities of each oxide by Kopp's Law,

$$C_p = \sum_i X_i C_{p_i} \qquad\qquad \text{(VI.2-3)}$$

where X_i is the mole fraction and C_{p_i} is the heat capacity of the ith component of the melt[34]. Using this relationship, the dependence of the heat capacity on the lime to silica ratio was determined. Because there was no relevant information in the literature on the effect of the lime to silica ratio on the speed of sound in liquid glass, the speed of sound was assumed to be constant.

The thermal conductivity of a glass of lime to silica ratio equal to B, $K_c(B)$, could be compared to a glass whose lime to silica ratio equaled unity, $K_c(1)$, using Equation (VI.2-1).

$$\frac{K_c(B)}{K_c(1)} = \frac{C_p(B) \, L(B)}{C_p(1) \, L(1)} \qquad\qquad \text{(VI.2-4)}$$
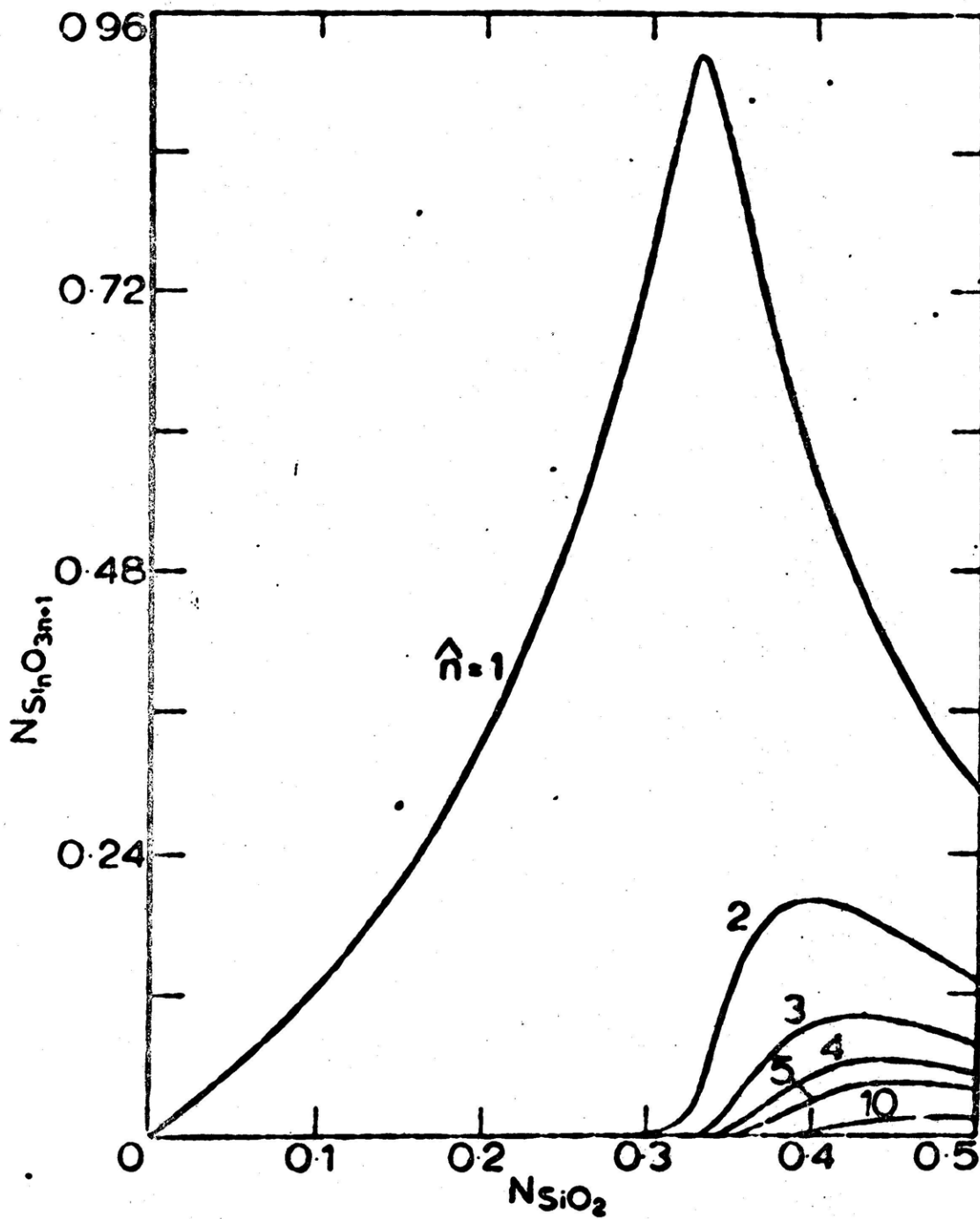
Figure VI.2-1 Calculated ionic distributions in $CaO-SiO_2$ melts at 1600°C (after Masson, Reference 31).

A straight line was fit to the calculated results of Equation (VI.2-4) and the relationship between K_c and B was found to equal

$$\frac{K_c(B)}{K_c(1)} = 1.5 - 0.5B \qquad \text{(VI.2-5)}$$

This relationship is shown in Figure VI.2-2. The associated error was ±10% for all of the data points between B equal to one and two. For B greater than two, this relationship is not valid.

As will be shown in more detail in Section VI.2-3, the values predicted by this correlation are in good agreement with the experimental results. For glasses #6 and #7, the measured values of k_{eff} were 3.0 X 10^{-3} cm²/sec at 1653°K and 2.4 X 10^{-3} cm²/sec at 1603°K, respectively. The predicted values of k_{eff}, when Equation (VI.2-5) is inserted into the correlation developed in Section VI.2.3, are equal to 3.4 X 10^{-3} and 2.6 X 10^{-3} cm²/sec, respectively.

A correlation which relates the thermal conductivity to the density of glass has been developed by Ratcliffe[35] for the temperature range -100°C to 150°C. In this temperature range the thermal conductivity as well as the density are functions of temperature. Consequently, it is possible to relate the thermal conductivity to the density. At higher temperatures where the thermal conductivity remains constant, the density continues to decrease. A correlation between the thermal conductivity and density of the type proposed by Ratcliffe,

$$K_c = \frac{a}{\rho} + b \qquad \text{(VI.2-6)}$$
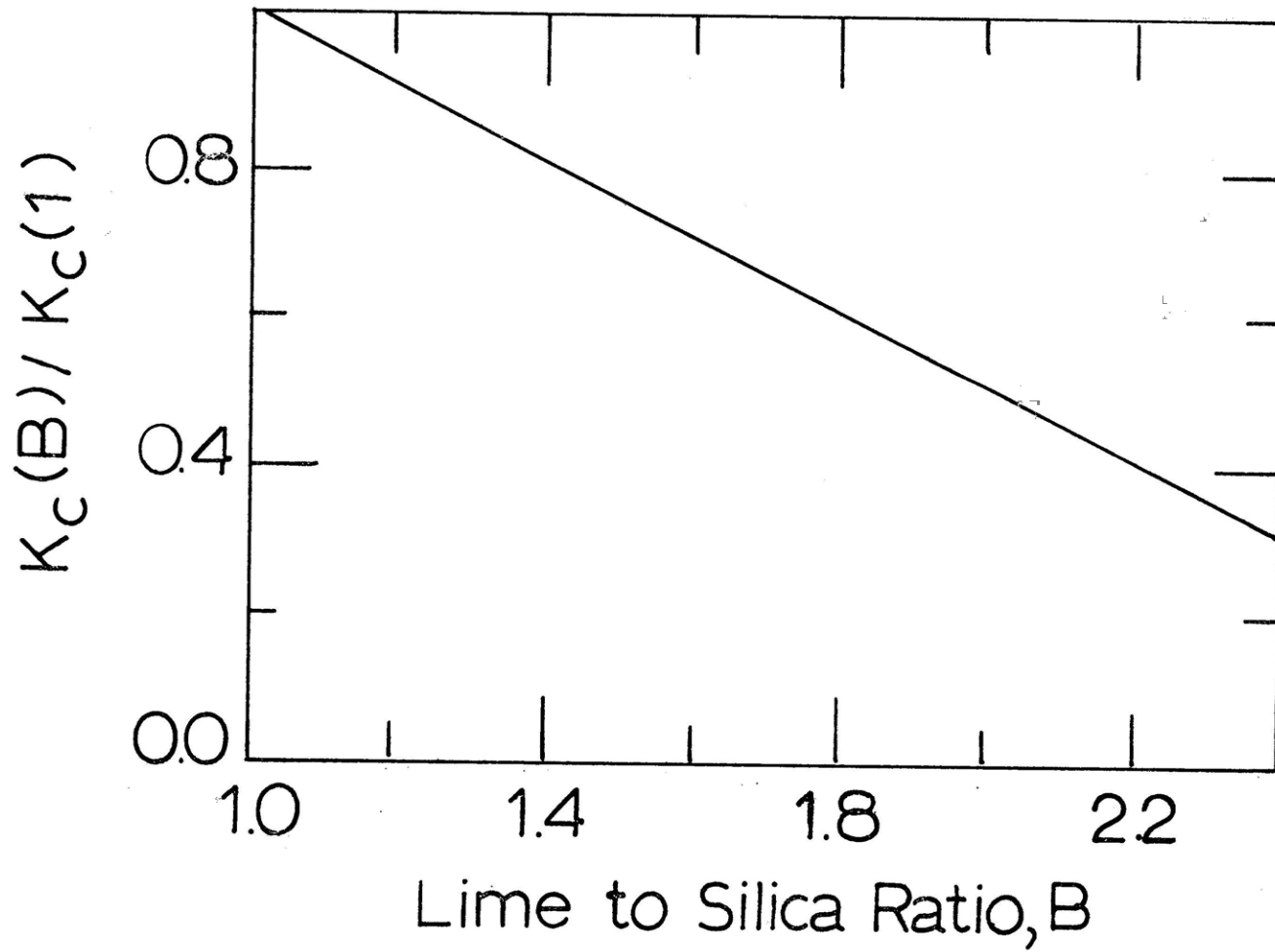
Figure VI.2-2   The predicted dependence of the thermal conductivity, K_c, on the lime to silica ratio, B.

where a and b are constants, in this case, is not likely.

VI.2.2   Radiation Conductivity

The radiation conductivity of a diathermanous material is defined in Section II.1 by Equation II.1-10,

$$K_r = \frac{16}{3} n^2 \, \sigma F T^3 \qquad\qquad (II.1-10)$$

To determine the dependence of K_r on the temperature and composition of the glass, the variation of the index of refraction, n, and the main free path of a photon, F, with temperature and composition must be known.

The variation of the mean free path of a photon, F, with temperature is the result of two effects. As noted in Section VI.1.1, the absorption spectrum of glass is a function of temperature. Consequently, as the temperature changes, the changing values of α_λ produce a variation in the value of F. However, even if the absorption spectra remained constant, the value of F would still be a function of temperature, because the wavelength distribution, β^*, used to calculate F is a function of temperature, see Table II.1-1. For glasses which contain FeO, the absorption spectrum decreases about 10% for a temperature change from 20°C to 1300°C, see Section VI.1.1. While the change in the absorption spectrum for temperatures has not been measured for higher temperatures, a similar rate of decrease in the absorption spectrum with increasing temperature can be assumed to occur. For glasses which contain large amounts of FeO, this decrease in the absorption spectra will be counterbalanced by the wavelength distribution shifting towards the strongest absorption band at 1.05 μm. For glass #3a (14.2% FeO), the largest contribution to the value of F was produced by the

wavelength band between 2.5 μm and 7.0 μm where α_λ was less than 100 cm^{-1}. For a temperature increase from 1500°K to 2000°K, the percentage of energy in this wavelength region will decrease from 49.3% to 32.9%. For the same temperature change, the percentage of energy in the wavelength band of greatest absorption, below 2.5 μm, increases from 43.3% to 63.4%[1]. Therefore, these two effects tend to cancel and result in a value of F that is independent of temperature.

Because the values of the index of refraction for the glass used in this investigation have not been measured, it is not possible to determine the effect of composition or temperature on this quantity. The indices of refraction of many other glasses have been determined and are nearly equal[36], so a constant value is assumed for the glasses being studied in this investigation. Consequently, since the mean free path of a photon, F, and the index of refraction, n, are not functions of temperature, the radiation conductivity of the glasses studied in this investigation are a function of the absolute temperature to the third power, as shown in Equation (II.1-10).

The absorption spectra for almost all glasses show complete absorption for energy at wavelengths greater than 4.75 μm[8]. Accordingly, the mean free path of a photon can be effected only by elements whose absorption spectra lie in the range below 4.75 μm. Of all of the oxides whose absorption spectra are in this range, the strongest absorber is FeO[13]. As shown by Kumugi and co-workers[37], even very small changes in the concentrations of FeO from 0.15% FeO to 0.30% FeO greatly reduce the radiation conductivity from 0.021 to 0.011 cal/cm sec °C. Since this oxide has such

a large effect on the radiation conductivity, the percentage of FeO will be dominant in determining the effect of composition on the radiation conductivity. The presence of other oxides and impurities in the melt will effect the radiation conductivity only by changing the equilibrium ratio of ferrous to ferric ions.

For many oxides, the absorption spectrum of the oxide is linearly dependent on the concentration, C_m, of the oxide in the glass being investigated,

$$\alpha_\lambda = \alpha_{\lambda m} \, C_m \qquad\qquad (VI.2-7)$$

This relationship is known as Bouguer's Law and $\alpha_{\lambda m}$ is the molar absorption coefficient. From the data available in the literature, two contradictory conclusions can be drawn for the applicability of this law for FeO. For silicate glasses, Steele[38] has found that a molar absorption coefficient equal to 28.9 L mole^{-1} cm^{-1} can be used to determine the absorption coefficient in the band at 1.05 μm. Weyl[13] has also shown that the absorption at this wavelength is linear in composition. Although Weyl did not report the concentrations of FeO in the glasses studied, these values can be calculated using 28.9 L/mole^{-1}cm^{-1} for the molar absorption coefficient. The results reported by Weyl are then found to be linear up to 2 moles/ liter of FeO. This equals 3.6% FeO in a glass similar to those being investigated here. On the other hand, Coenen[12] has suggested that for the glasses which contained up to 4% Fe_2O_3, melted under reducing conditions, the absorption coefficient was proportional to (% FeO)$^{1/4}$. Coenen concluded on this basis that FeO does not obey Bouguer's Law and that the failure to obey the law is a result of the fact that iron oxide in the

glass may be in both the ferrous and ferric states. Since the ratio of ferric to ferrous ions in the melt can change with temperature, a molar absorption coefficient for total iron is not correct. If Coenen had analyzed for FeO rather than total iron as FeO or Fe_2O_3, his results would probably agree with Steele and Weyl.

Using the molar absorption coefficient equal to 28.9 L mole^{-1} cm^{-1}, $\alpha_{1.05 \ \mu m}$ for glass #2 which contained 6.3% FeO (3.5 moles/L) should be equal to 105 cm^{-1}. The measured value of 150 cm^{-1} indicates that at higher values Bouguer's Law is not valid for FeO. The dependence of the absorption on the percentage of FeO is of higher order than one, as the actual result is larger than the value predicted by Bouguer's Law. With this very limited data, it is not possible to determine the exact relationship between the absorption and the percentage of FeO. The available information does indicate that the absorption coefficient is proportional to (% FeO)^p where p is greater than one. Consequently, since the mean free path is determined from the inverse of the absorption spectra, F will be inversely proportional to (% FeO)^p.

Combining the effect of temperature and composition on the radiation conductivity to obtain a general result, the radiation conductivity will equal

$$K_r = K \ T^3/(\% \ FeO)^p \qquad\qquad (VI.2-8)$$

where K and p are constants.

VI.2.3 Effective Thermal Diffusivity

Using the relationships presented in Sections VI.2.1 and VI.2.2,

a correlation is developed to relate the experimentally determined values of the effective thermal diffusivity to the composition and temperature of the glasses investigated. The degree of fit and the associated error of this correlation are discussed. Several alternative relationships are also presented.

As shown in Section II.1, the effective thermal diffusivity is related to the effective thermal conductivity by the product of the density and heat capacity of the medium[7],

$$k_{eff} = K_{eff} / \rho\, C_p \qquad\qquad (II.1\text{-}12)$$

Although the density and heat capacities of the glasses being investigated have not been determined, it is generally found that the heat capacity increases slightly with increasing temperature[34], while the density decreases[32]. The result is a nearly constant product. Assuming that the product is constant, the effective thermal diffusivity will equal a constant times the effective conductivity, and

$$k_{eff} = f_1(B) + f_2(T^3, \%\ FeO^{-p}) \qquad\qquad (VI.2\text{-}9)$$

where

$$f_1(B) = \frac{k_c(1)}{\rho\, C_p} (1.5 - 0.5\ B) \qquad\qquad (VI.2\text{-}9)$$

$$f_2(T, \%\ FeO^{-p}) = \frac{K}{\rho C_p} \frac{T^3}{(\%\ FeO)^p} \qquad\qquad (VI.2\text{-}10)$$

and K and p are constants. For glasses with a constant lime to silica ratios, Equation (VI.2-6) reduces to the form:

$$k_{eff} = a + b \frac{T^3}{(\% \, FeO)^p} \qquad\qquad (VI.2-11)$$

where a, b and p are constants. Using the minimum sum of squared devia-
tions as the criterion for determining the best fit[25], several relation-
ships were fitted to the experimentally determined values of effective
thermal diffusivity. The values of p that were tried were 1/4 (the value
suggested by Coenen), 1/2, 1, 1.5 and 2.0. While a significant difference
did not exist between the degree of fit for p equal to 1/2, 1, 1.5 or 2.0,
it is shown that p equal to 1/4 produces a significantly lower degree of
correlation, see Table VI.2-1.

For p equal to 1/4 and 1/2, the predicted thermal conductivities were
negative. Since these results have no physical meaning, these correlations
can be disregarded. For the three remaining correlations, the values of
the radiation diffusivity were calculated for glass containing 12.6% FeO
(#3a) at 1300°C. The calculated values were 1.7×10^{-3}, 1.3×10^{-3} and
0.8×10^{-3} for p equal to 1, 1.5 and 2.0, respectively. Comparison of
these values with the calculated value of the radiation conductivity is
only possible if the product of ρC_p is known. This value is assumed to be
between 0.8 and 1.0 cal/cm³ °C, and the radiation diffusivity determined
from the absorption spectrum is equal to 0.9 to 0.7 cm²/sec.

The agreement between the value predicted by the correlation for p
equal to two and the calculated value from the absorption spectra is excel-
lent. The value of the thermal diffusivity predicted by this correlation
is also in good agreement with the values predicted by other investiga-
tors[26,7]. Consequently, this correlation can be used to represent

TABLE VI.2-1

The Correlations and the Resulting Correlation
Coefficients That Were Fit to the Experimental Results

Correlation	Correlation Coefficient, r
$k_{eff} \times 10^3 = -1.49 + 7.86 \frac{(T/1500)^3}{(\% \ FeO)^{1/4}}$	0.8
$k_{eff} \times 10^3 = -5.50 + 26.78 \frac{(T/1500)^3}{(\% \ FeO)^{1/2}}$	0.92
$k_{eff} \times 10^3 = 0.75 + 32.55 \frac{(T/1500)^3}{(\% \ FeO)}$	0.95
$k_{eff} \times 10^3 = 1.59 + 86.3 \frac{(T/1500)^3}{(\% \ FeO)^{3/2}}$	0.93
$k_{eff} \times 10^3 = 2.38 + 200.7 \frac{(T/1500)^3}{(\% \ FeO)^2}$	0.92
$k_{eff} \times 10^3 = 1.72 + 323.9 \frac{(T/1500)^2}{(\% \ FeO)^2}$	0.95
$k_{eff} \times 10^3 = 3.78 + 2.52 \frac{(T/1500)^4}{(\% \ FeO)^2}$	0.10

accurately the measured values of the effective diffusivity. The maximum error limits for a predicted value of k_{eff} were calculated for 95% and 99% confidence limits[25], and were equal to $\pm 0.5 \times 10^{-3}$ and $\pm 0.7 \times 10^{-3}$ cm²/sec., respectively.

Correlations were also fit to the data for other powers of the absolute temperature. As shown in Table VI.1-1, the fit for the correlation versus T^4 was significantly lower than for T^3, while there was no significant difference between the degree of correlation for T^3 and T^2. As would be expected because of the high correlation coefficient for both correlations, the predicted values of both curves were within $\pm 0.5 \times 10^{-3}$ cm²/sec for all values of % FeO between 10 and 25% and temperatures up to 2000°K. However, because the correlation versus T^3 is in agreement with the dependence of the radiation conductivity predicted in Section VI.2.2, the correlation,

$$k_{eff} \times 10^3 = 2.38 + 200.7 \frac{(T/1500)^3}{(\% \text{ FeO})^2} \qquad \text{(VI.2-12)}$$

is assumed to be the best possible representation of the measured results. The correlation and results are shown in Figure VI.2-3.

To generalize Equation (VI.2-12) to include the effect of the lime to silica ratio, B, on the thermal conductivity, Equation (VI.2-9) must be combined with the correlation. The resulting relationship equals

$$k_{eff} \times 10^3 = 2.38 (1.5 - 0.5 B) + 200.7 \frac{(T/1500)^3}{(\% \text{ FeO})^2} \quad \text{(VI.2-13)}$$

Using this correlation, the values of k_{eff} for glass #6 at 1653°K, and glass #7 at 1603°K were calculated to be 3.0×10^{-3} and 2.4×10^{-3} cm²/sec,
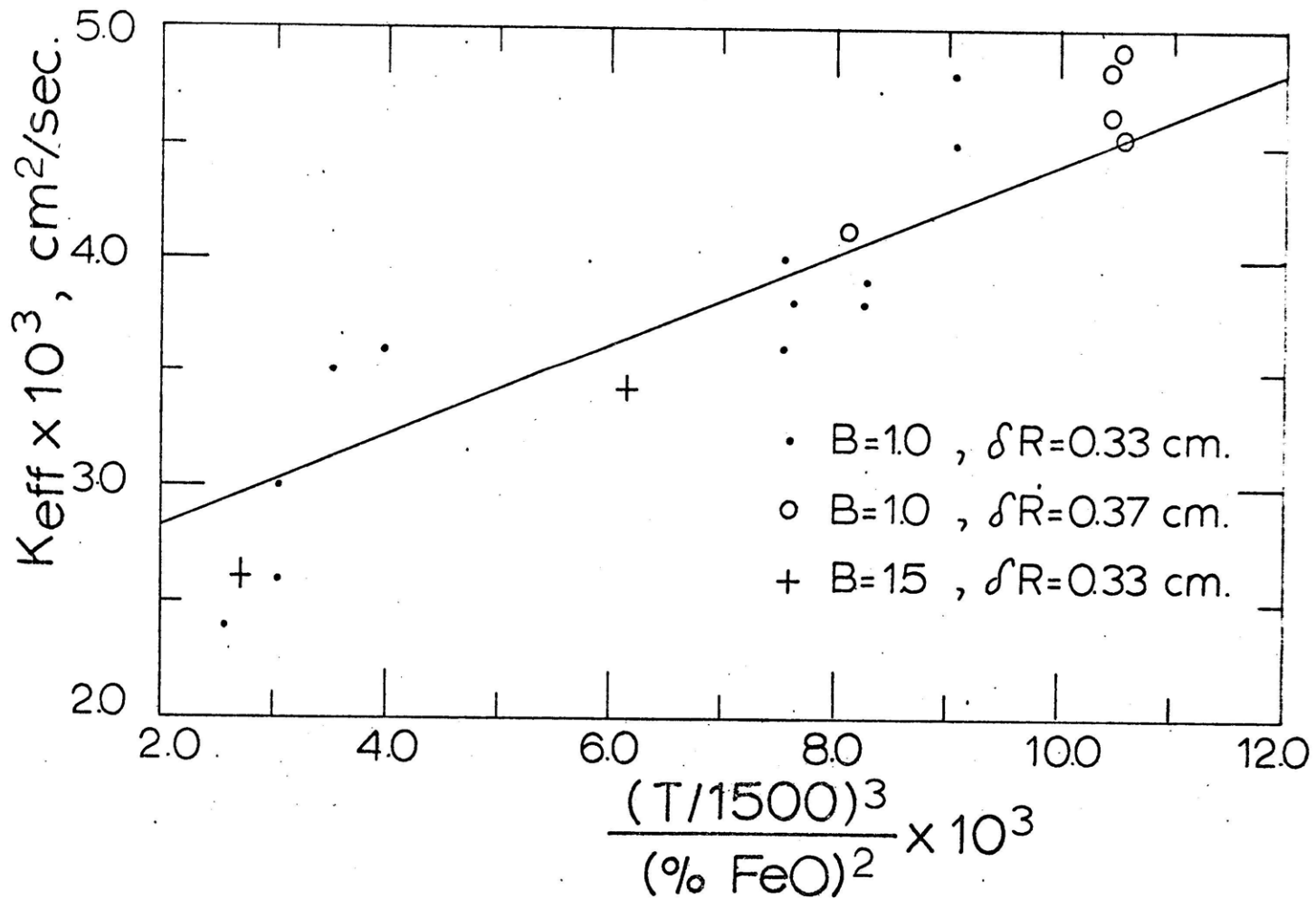
Figure VI.2-3   The experimental results and correlation which relates the effective thermal diffusivity to percent FeO and temperature.

respectively. These calculated values are in very good agreement with the measured values of 3.4 X 10^{-3} and 2.6 X 10^{-3} cm^2/sec. It is therefore concluded that Equation (VI.2-13) can be used to predict the effect of the lime to silica ratio, B, as well as the effects of temperature and composition on the effective thermal diffusivity of liquid glasses similar in composition to metallurgical slags. As noted in the development of Equation (VI.2-5), this equation is only valid for B between 1 and 2. Consequently, Equation (VI.2-13) should also be limited to lime to silica ratios between 1 and 2.

Finally, since the measured values for the large (δR = 3.7 mm) and small (δR = 3.3 mm) crucibles agree with the correlation, the assumption made in Appendix B of an optically thick glass sample is confirmed.

The correlation developed in this section to relate the effective thermal diffusivity to the composition and temperature of the glass, has been derived from the theoretical treatment of the dependence of the thermal conductivity and radiation conductivity on composition and temperature. This correlation fits the experimental results remarkably well, and consequently, can be used to extrapolate these results to other glass compositions and temperatures.

VII. PRACTICAL IMPLICATIONS OF THE STUDY

Heat transfer in the slag layer in a metallurgical furnace can occur by conduction, radiation and convection. In this chapter, a surface renewal model based upon a model proposed by Danckwerts[39] is presented to describe convective heat transfer in a slag layer in an electric furnace. The results of this model are compared with the heat flow predicted for conduction and radiation in a stagnant slag layer to determine the rate limiting steps of the heat transfer processes occurring within the slag.

In the surface renewal model, an element of slag is brought by convection from the interior of the slag layer to the surface. Once at the surface, the layer is exposed to a net heat flux, q_{in}, from the chamber surrounding it. The element is then mixed back into the interior of the slag, producing a new surface and resulting in a net heat transfer to the bulk slag, see Figure VII-1.

For an element of slag of thickness x and unit area at the surface of slag layer, the change in mean temperature, $\overline{T}$, with time equals

$$x\rho C_p \frac{\partial \overline{T}}{\partial t} = q_{in} - q_{out} \qquad \text{(VII-1)}$$

where q_{in} will equal the net heat flux from the surroundings and q_{out} will equal heat loss due to conduction and radiation into the melt.

To make the mathematical model more tractable, the following assumptions were made:

1) The heat flux from the surroundings to the surface for a slag layer that is being stirred is much larger than the heat flux by conduction and
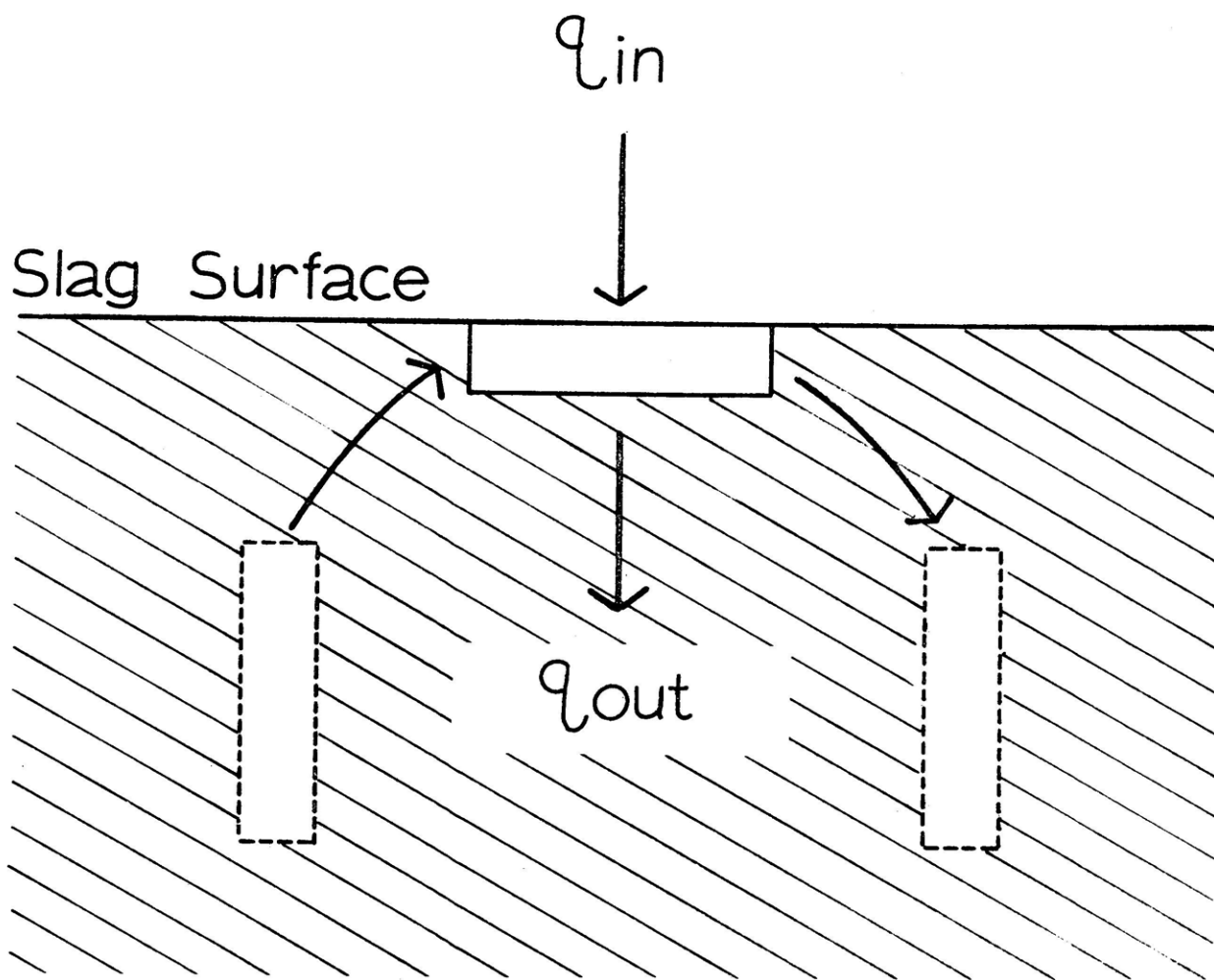
Figure VII-1 A schematic representation of the mass flow
and heat fluxes described by the surface renewal model.

radiation from the element to the bath,

$$q_{in} \gg q_{out} \qquad (VII-2)$$

2) The radiation heat flux to and from the surface can be linearized[40] and is of the form

$$q_{in} = h_r (T_\infty - \overline{T}) \qquad (VII-3)$$

3) The surface element is not mixed. However, since the element is diathermanous, it is assumed that x is equal to the depth of penetration of incident energy. Also, the energy is absorbed uniformly throughout the element.

4) The probability of a surface layer being renewed is independent of the length of time, t, it has been on the surface.

When assumptions 1) and 2) are applied, Equation (VII-1) becomes

$$\frac{\partial \overline{T}}{\partial t} = \frac{(T_\infty - \overline{T})}{\tau} \qquad (VII-4)$$

where

$$\tau = \frac{x \rho C_p}{h_r} \qquad (VII-5)$$

τ is equal to the thermal time constant of the surface element. For the initial condition,

$$t < 0, \ \overline{T} = T_B \qquad (VII-6)$$

where T_B is the bulk slag temperature, the solution to Equation (VII-4) is equal to

$$\frac{T_\infty - \overline{T}}{T_\infty - T_B} = e^{-(t/\tau)} \qquad \text{(VII-7)}$$

Substituting Equation (VII-7) into Equation (VII-3),

$$q_{in} = h_r(T_\infty - T_B) \, e^{-(t/\tau)} \qquad \text{(VII-8)}$$

As shown by Donckwerts[39], the fraction of the surface covered by elements of age between t and t + dt is equal to Se^{-St} dt. For this distribution, the heat flux to the fraction of the surface of age between t and t + dt is equal to

$$h_r(T_\infty - T_B) \, e^{-(t/\tau)} \, Se^{-St} \, dt$$

and the average flux, Q, to the surface is then equal to

$$Q = \int_0^\infty h_r(T_\infty - T_B) \, S \, e^{-(\frac{1}{\tau} + S)t} \, dt \qquad \text{(VII-9)}$$

Performing the integration,

$$Q = h_r(T_\infty - T_B) \, \frac{S}{(\frac{1}{\tau} + S)} \qquad \text{(VII-10)}$$

and,

$$\frac{Q}{h_r(T_\infty - T_B)} = \frac{S\tau}{1 + S\tau} \qquad \text{(VII-11)}$$

This relationship between the dimensionless flux and $S\tau$ is shown in Figure VII-2.

The results predicted by the model are intuitively consistent. For small values of $S\tau$, the mean residence time of an element, 1/S, is much
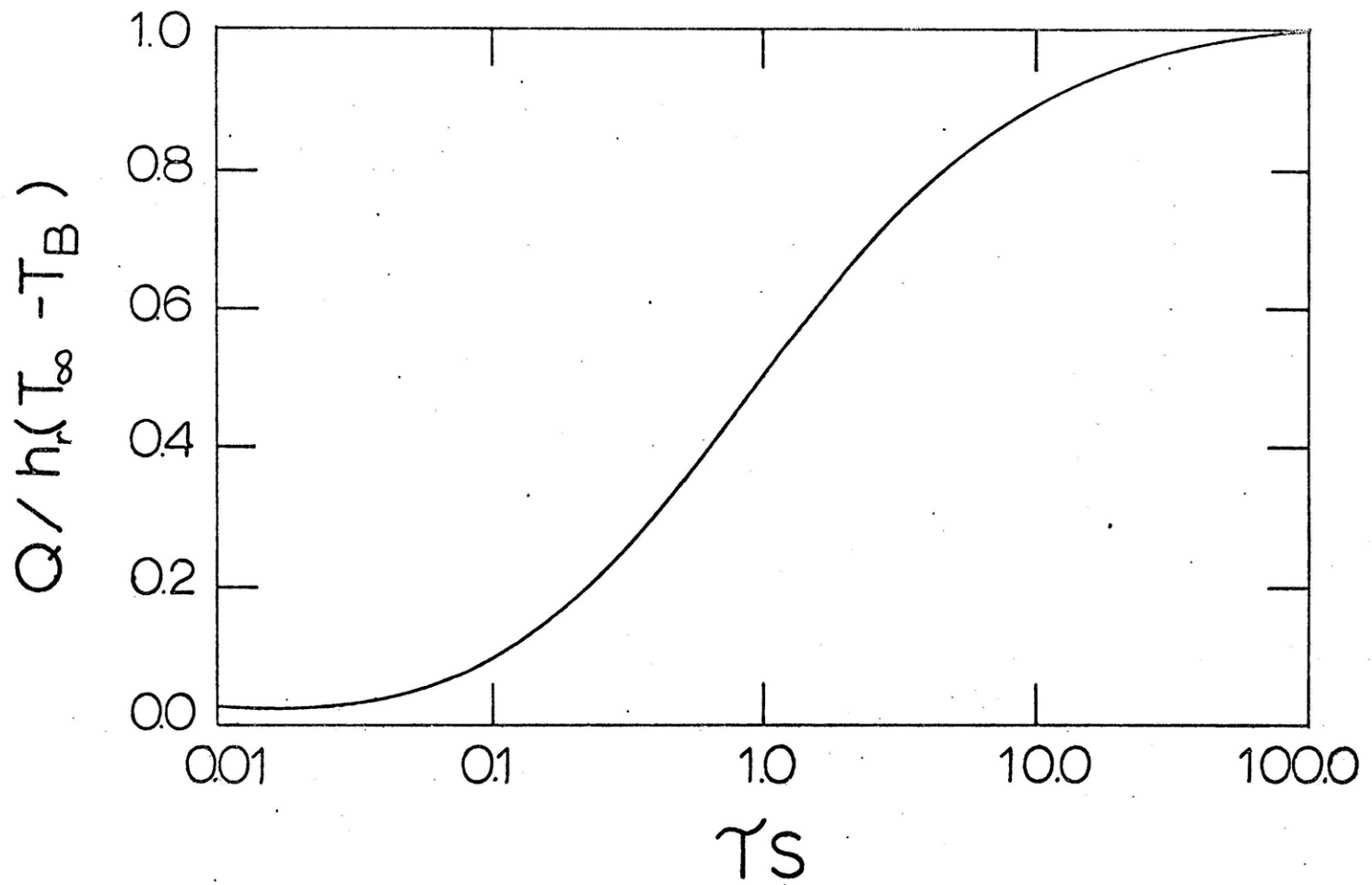
Figure VII-2   The relationship between the dimensionless heat flux, $Q/h_r(T_\infty - T_B)$, and the parameter τS predicted by the surface renewal model.

larger than the thermal time constant, τ, and convection controls the rate
of heat transfer. For large values of $S\tau$, the time constant is large
compared to the residence time, and heat transfer to the surface is the
limiting factor. For an infinite mean residence time, there is no convec-
tion, $S\tau$ equals zero and the model predicts no heat transfer. This result
is produced by assumption number (1).

To apply this model to the chamber of an electric furnace, an average
chamber temperature, $\overline{T}_\infty$, must be determined. The total flux to the sur-
face will be composed of the flux from the arc, $\sigma \, \varepsilon_{arc} \, T_{arc}{}^4$, and the flux
from the chamber, $\sigma \, \varepsilon_\infty T_\infty{}^4$. The average temperature, $\overline{T}_\infty$, will then be
defined by

$$\sigma \, \varepsilon_\infty \overline{T}_\infty{}^4 = \sigma \, \varepsilon_{arc} F_{arc-1} T_{arc}{}^4 + \sigma \, \varepsilon_\infty F_{\infty-1} T_\infty{}^4 \quad (VII\text{-}12)$$

and

$$\overline{T}_\infty = (\varepsilon_{arc} F_{arc-1} T_{arc}{}^4 + \varepsilon_\infty F_{\infty-1} T_\infty{}^4)^{0.25}/\varepsilon_\infty \quad (VII\text{-}13)$$

The values of $(T - T_B)$ and h_r were calculated for normal operating condi-
tions[41,42], and were equal to approximately 100°K and 0.03 cal/cm²sec,
respectively.

The heat flow due to conduction and radiation in a stagnant layer was
found by assuming that a temperature drop of 100°K existed over a slag
layer 30 cm thick[43]. For a slag containing 20% FeO and with a lime to
silica ratio equal to 2, the effective thermal diffusivity for an average
slag temperature of 1900°K was equal to 3.0×10^{-3} cm²/sec, see Equation
(VII.2-9). The product ρC_p was assumed to equal 1 cal/cm³°C. For a stag-
nant slag layer, the dimensionless flux is equal to the flux due to

conduction and radiation, Q_c, divided by $h(T_\infty - \overline{T})$. For the conditions previously described,

$$\frac{Q_c}{h(T_\infty - \overline{T})} = \frac{k_{eff} \, \Delta T / \Delta X}{h(T_\infty - \overline{T})} = 0.003 \qquad \text{(VII-14)}$$

The value of $Q_c/h(T_\infty - T_B)$ can then be added to the values of $Q/h(T_\infty - T_B)$ to obtain an approximation of the combined effect. This correction, however, does not significantly change the results predicted by the surface renewal model. At low values of $S\tau$, heat transfer in the slag layer is still controlled by conduction, radiation and convection within the layer. For large values of $S\tau$, the heat transfer process within the slag is limited by the rate at which heat arrives at the surface. Consequently, it can be concluded that the rate of heat transfer from the furnace chamber through the slag layer to the iron pool below is mainly a function of degree of agitation of the slag. Under stagnant conditions, the amount of heat transfer through the layer is small, and the chamber temperature should therefore be high. For stirred slag layers, the heat transfer through the slag layer increases and the chamber temperature should be lower than for a stagnant bath. In actual electric furnace operation[43], the above mentioned phenomena do occur. During the production of a single heat of steel, the furnace chamber temperature increases quite dramatically if the slag layer becomes quiescent. If stirring is again produced, the chamber temperature drops.

Although the stirring parameter, S, cannot be easily measured for any metallurgical system, the model derived in this section is still of value. The model can be used to characterize the effect of stirring on heat

transfer in slag baths and hence, the importance of convection as compared with conduction and radiation in a stagnant bath.

VIII. SUMMARY AND CONCLUSIONS

An experimental technique has been developed for measuring the effective thermal diffusivity of liquid glasses similar in composition to metallurgical slags. This apparatus was used successfully to measure the diffusivity of glasses which contained between 11 and 25 wt. % FeO. The lime to silica ratio of the glasses varied from 1.0 to 1.5 and the temperature range investigated was from 1300°C to 1500°C.

A correlation was developed to interpolate values of the effective thermal diffusivity within the experimentally investigated range of temperature and composition. The associated error of the correlations was ±10%. The correlation also allows extrapolation of the experimental results to other compositions and temperatures with approximately the same error.

Unlike iron free glass, where the radiation conductivity is approximately 50 times the thermal conductivity, the radiation and thermal conductivities of glasses similar in composition to metallurgical slags are of the same order of magnitude. As shown by the correlation fit to the experimental data,

$$k_{eff} \times 10^3 = 2.38 \ (1.5 - 0.5 \ B) + 200.6 \ \frac{(T/1500)^3}{(\% \ FeO)^2} \quad (VI.2\text{-}13)$$

at low temperatures and high percentages of FeO, the thermal conductivity is larger than the radiation conductivity. At high temperature and low FeO concentrations, the radiation conductivity is larger. There are no conditions for which one mode of heat transfer dominates over the other.

IX. SUGGESTIONS FOR FUTURE WORK

While a suitable method for measuring the effective thermal diffu-
sivity of glasses similar in composition to metallurgical slags has been
developed, the range of glass compositions investigated has been limited to
the relatively low melting point of the iron crucibles used on the ap-
paratus. To increase the range of temperatures for which experiments can
be performed, a different crucible material should be found.

Molybdenum has been suggested as a possible container for glasses
which contain iron. This material has a much higher melting point,
$2610°C$[50], than does iron, while it has approximately the same equilibrium
oxygen potential. Glasses used in crucibles made of molybdenum should be
prepared in larger crucibles made of molybdenum so that the equilibrium
concentration of MoO_2 will be present in the glass being investigated.
This amount is reported to be approximately 1%[51], and should not effect
the measured effective diffusivities to any great extent.

Several other problems will also have to be overcome to perform these
experiments. The alumina tubes used to insulate the molybdenum wire from
the crucible and glass will dissolve much faster at higher temperatures.
Either a different material will have to be found or a molybdenum coating
will have to be applied to the alumina tube to prevent the dissolution
process. There may also be new problems produced in the method for pre-
paring the long cylindrical samples. Quenching glasses from higher tem-
peratures may produce such large strains that the samples shatter.

It would be of great value to perform experiments with glasses of

higher lime to silica ratios and at higher temperatures using the modifications to the apparatus previously mentioned. However, these experiments will be extremely difficult to perform because of the high temperatures required and the associated materials problems.

The apparatus described in Section IV.2 with minor modifications can also be used to measure the effective thermal conductivity of liquid glasses. By replacing the molybdenum wire with a thermocouple, the temperature at the center of the glass sample could be measured. If a known power were passed through this wire and the temperature at the inside and outside of the crucible measured at steady-state, the effective thermal conductivity could be found from the equation for steady-state radial heat transfer in a cylinder. For these experiments, it would also be necessary to either replace or protect the alumina tube which surrounds the molybdenum wire, as these experiments would necessitate a much longer experiment life than the periodic steady-state method currently being used[52].

With this information and the results of periodic steady-state measurements, it would be possible to determine the values of the product ρC_p for the glasses as a function of temperature. Using a maximum bubble pressure technique[53], the density could be found, and hence the heat capacity could be determined.

Finally, it would be extremely useful if a technique could be developed for measuring the absorption spectra of liquid glasses containing large amounts of FeO. Using this information, more accurate correlations could be developed for the measured values of the effective thermal conductivities and diffusivities. This would permit a more accurate prediction

of these quantities for glass composition and temperatures which have not been measured. Presently available techniques are not applicable because the iron will destroy the platinum mirror used in Genzel's apparatus[10] and the synthetic sapphire windows incorporated into Grove's technique[11]. A new method for measuring the absorption spectrum would have to overcome this ever present materials problem.

APPENDIX A

PRELIMINARY EXPERIMENTAL METHODS FOR MEASURING EFFECTIVE
THERMAL DIFFUSIVITY OF LIQUID GLASS

Several methods were tried for measuring the effective thermal diffusivity of liquid glass samples before the technique currently being used was developed. These methods will be described briefly, and their main experimental difficulties discussed.

A small furnace consisting of two small platinum strip heaters was initially used in an attempt to measure k_{eff} of liquid glasses. The heaters were positioned in a manner which produced a hot zone approximately 6 mm by 6 mm with a variable thickness, see Figure A-1. Thermocouple supports were positioned on moveable stages so that a thermocouple could be placed at a known position within the hot zone. The heaters and thermocouple were held in tension so that their position would not change during heating and cooling.

A small glass sample was placed in the furnace and heated to a steady-state temperature. Using the potentiostat and function generator described in IV.2, the temperature of the heaters was varied in a systematic manner in time. By measuring the phase-shift in the response of the thermocouple, the effective thermal diffusivity of the liquid glass could be found.

For this technique, it was necessary to make small butt-welded thermocouples. The thermocouples had to be small compared to the thickness of the glass sample (approximately 2.5 mm), thus a maximum thermocouple thickness of 0.05 mm was allowable. It was not possible to weld these thermocouples using ordinary welding methods because of their extremely small
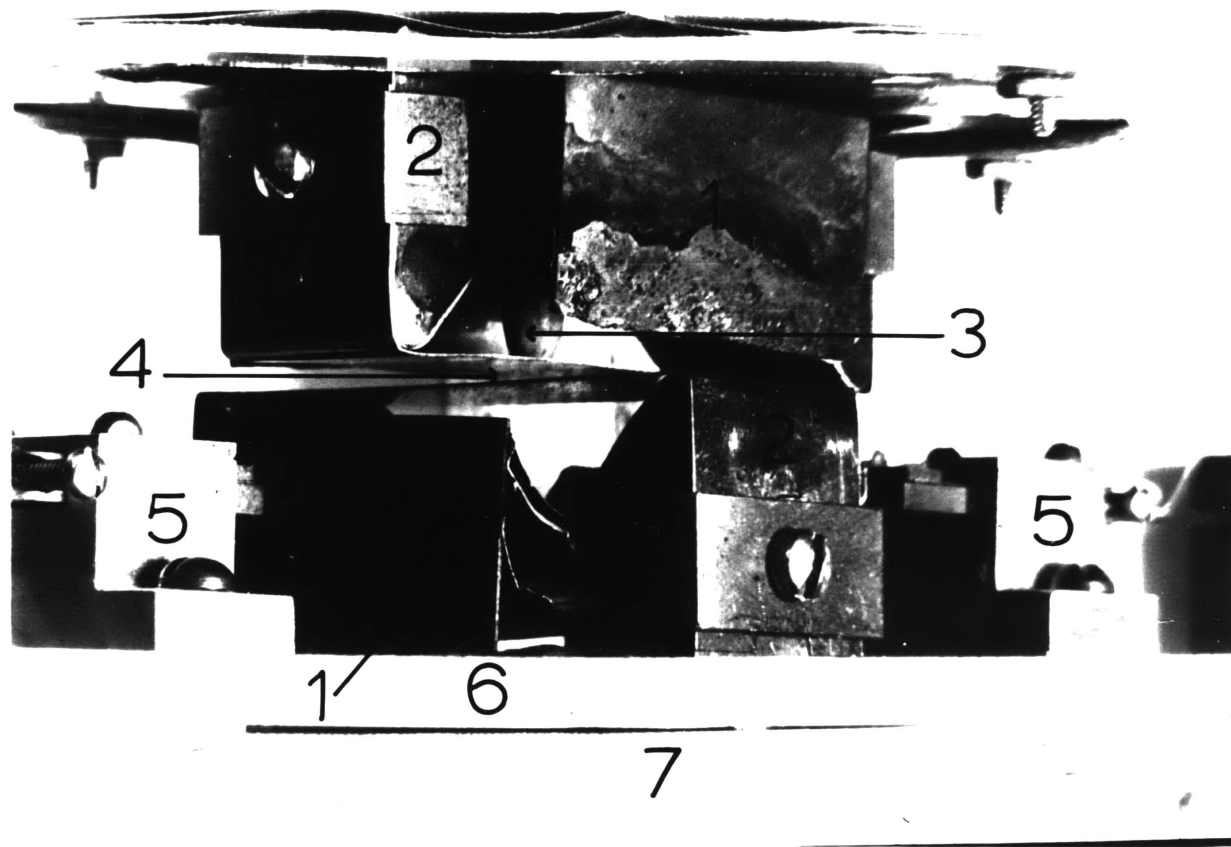
Figure A-1   Photograph of initial apparatus used for measuring the effective thermal diffusivity of liquid glasses. (1) radiation heat shields, (2) bus bars, (3) light pipe, (4) strip heaters, (5) thermocouple supports, (6) moveable stage, (7) bus bar support.

size. The only suitable method for preparation was to electron beam butt-weld a 0.05 mm thick sheet of platinum to a sheet of Pt-10% Rh of the same size. Thermocouples 0.25 mm wide by 10 cm long, and 0.05 mm thick then were sheared from the welded sheets.

The platinum heaters were made by spot welding a strip of 0.05 mm thick by 6 mm wide platinum foil to heavier platinum supports. These supports were fastened to copper bus bars which were supported in bakelite fixtures. Radiation shielding was positioned around the heaters to minimize the heat losses. A current of approximately 60 amperes was required to reach a steady-state temperature of 1300°C. Temperatures up to 1500°C could be attained.

For this technique, it was critical that the sample thickness and thermocouple position be measured accurately. These distances were measured using a Bausch and Lomb stereo microscope. However, because of the nature of the bus bar supports, it was possible for the strip heaters to become askew during experiments. This problem was not correctable, so a new furnace was built.

The new apparatus was very similar to the initial furnace with two exceptions. From the results of the study on the absorption spectra of these slags, it was determined that a minimum sample thickness of 2 to 3 mm was required. Therefore, in order that one dimensional heat transfer be assured along the axis of a cylindrically shaped sample, a larger sample diameter was necessary. The hot zone of the new furnace was approximately 13 mm square, and also permitted use of slag samples of a range of thicknesses. Also, the bus bars in this apparatus were mounted in Teflon in a

manner which allowed their position to be adjusted so that the heaters remained parallel during the experiments.

The experimental difficulties associated with this technique were numerous. These difficulties can be grouped into four major areas; problems with the electrical heating and measuring systems, mechanical problems, sample preparation problems, and chemical problems.

Because of the small size of the furnaces and samples used in these experiments, the temperature was very sensitive to minor variations in the heating current. This sensitivity had been designed into the apparatus so that diffusivity measurements could be made quickly before the liquid glass attacked the thermocouples and heating elements. However, because of the large amperage required to heat the furnaces, it was very difficult to prevent the steady-state current from drifting. Large storage batteries were used as a current supply, and rheostats as regulators. However, because of the high currents through these rheostats, their temperature would change during experiments, resulting in a changing current. Several types of rheostats, wire wound as well as a carbon pressure sensitive type, were tried. The results were the same for all types. Oil cooling was used with little success in an attempt to prevent heating. This problem was finally solved by heating the rheostats to their steady-state temperature before the experiment began.

For these experiments, it was necessary to be able to measure temperature variations of approximately 1°C. For platinum versus Pt-10% Rh thermocouples, this small temperature variation produces approximately a 10 microvolt response. Several types of instruments, including

oscilloscopes, x-y recorders, and strip chart recorders were used to obtain a noise free signal from the thermocouples. The best results were obtained using chart recorders because of the mechanical damping associated with the lag in the pen and pen drive. However, these results were still not of the best quality.

The spring-loading systems which kept the heaters and thermocouples in position also produced many problems. It was very difficult to attain the exact amount of tension which would overcome the frictional forces of the mechanisms and not break the thin foils. This problem was especially critical for the thermocouples because of their small cross-sectional area (0.0125 mm^2). Several spring and pulley systems were tried to overcome this problem, however, a weight suspended on a thread was the best solution.

Because the current requirements for melting samples became much larger as the sample thickness increased, the densest possible solid glass samples were required to produce liquid samples of the desired size. Pill shaped samples were made by pressing thoroughly mixed reagent grade powders with and without a binder material. Samples were also made from powders which had been fused, crushed and pressed into pellets. Both of these methods resulted in very small liquid samples or larger annular samples, i.e. a ring of liquid around a large gas bubble. Samples were finally made by cutting rectangular pieces out of larger glass samples which were prepared in a manner similar to that described in IV.1. The densities of these samples were determined, and only the densest samples were used. Upon melting, the liquid glass formed a cylindrical sample within the hot zone of the furnace to minimize its surface energy.

Having solved the majority of the electrical, mechanical and sample preparation problems, experiments were begun on liquid glasses. Immediately, it became evident that the thermocouples could not be placed within the slag. Because the thermocouples were thin and completely surrounded by slag, alloying of the platinum with the iron in the glass occurred rapidly after the glass became molten[44]. This resulted in an erratically varying thermocouple potential and eventually melting of the iron-platinum alloy[45]. Also, an analysis of the electrical resistance of the liquid glass sample indicated that the resistance of the sample was of the same order of magnitude as the heaters (approximately 0.1 ohms). Because of the complex geometry of the potential fields across the two flat surfaces of the sample, a simplified analysis based upon a constant potential was applied. The resistance predicted by this analysis would be much smaller than the actual resistance. However, even if the actual resistance were 10^4 times larger, a current of several milliamperes would be passing through the samples. This current would also produce erroneous thermocouple potentials for unprotected thermocouples of any type placed in the melt.

Alternative methods for measuring the effective thermal diffusivity with this apparatus and thermocouples positioned outside of the melt were then studied. By oscillating the temperature of one heater and measuring the response of the other, it was also possible to determine k_{eff} of the melt. For these experiments, an IR-Tronics total emission pyrometer was used to measure the temperature of the upper heating element while the temperature of the lower element was oscillated sinusoidally. This measurement was made possible by using a synthetic sapphire rod which passed

through the bus bar supports and radiation shielding as a light pipe. To achieve a more reproducable temperature measurement, the total emission pyrometer was replaced by a Therm-O-Scope two color pyrometer. The outputs of these pyrometers were recorded using the same instruments as for the thermocouple output. Several experiments were performed on low melting glasses, such as soft glass and green bottle glass to obtain a temperature calibration for the pyrometer and a temperature-current curve for the furnace.

Experiments were then attempted using glasses containing 20 wt. % FeO. In these experiments, the platinum heaters lasted only a few minutes which was insufficient for making a measurement. These failures were also attributed to alloying of the platinum with the iron in the glass. However, for the case of the heaters, a different mechanism for the alloying process is possible. Because the liquid oxide is an ionic conductor, the transport of iron ions from the high potential to the lower potential heater occurs. Also at this lower potential heater, the iron ion is reduced to metallic iron which plates out onto the platinum. With this intimate contact, alloying progresses at a much faster rate. To overcome this problem, metallic foils which had little or no solubility of iron, such as molybdenum or tungsten were tried. An enclosure was built to provide a protective atmosphere for the furnace so that molybdenum could be used for the strip heaters[46]. However, with this arrangement, as soon as the glasses became liquid, the molybdenum began to react with the FeO in the glass and the heaters failed. The greatest excess was obtained with iron heaters. However, at 1300°C to 1400°C, these foils did not have enough strength to

be held in tension.

After performing approximately 100 experiments with these furnaces, this technique was abandoned and the apparatus described in Section IV.2 was built.

APPENDIX B

MATHEMATICAL ANALYSIS OF THE APPARATUS FOR MEASURING
THE EFFECTIVE THERMAL DIFFUSIVITY OF GLASSES

For radial periodic steady-state heat flow in an infinitely long hollow circular cylinder, the phase angle between the temperatures of two concentric surfaces is a function of their position and the thermal diffusivity of the cylinder. In this appendix, the analysis for radial periodic steady-state heat flow is applied to the apparatus for measuring the effective thermal diffusivity of liquid glass to determine the relationship between the measured phase angle and the diffusivity of the glass sample.

B.1 Analysis of Experimental Apparatus

In this investigation, a typical glass sample was 6 cm long, and either 0.37 or 0.42 cm in outer radius. Therefore, it was possible to assume that the sample was infinitely long, when the temperature measurement of the iron crucible wall was made at a point 3 cm from the bottom of the glass sample.

Because the thermal diffusivity of molybdenum is much larger than that of glass (approximately 10^4 times), and because the diameter of the wire was much smaller than that of the glass, it was assumed that the wire had a uniform temperature over its cross-section. Accordingly, the temperature of the wire is a function of time only, and a periodically varying current impressed on the wire will result in a periodically varying temperature at the inner surface of the small alumina tube, (Figure IV.2-1).

A matrix technique for the solution of the set of differential equations and boundary and initial conditions, that describe the radial periodic steady-state heat flow in an infinitely long composite cylinder, has been presented by Carslaw and Jaeger[47]. However, for the analysis of this experimental apparatus, each component of the alumina, liquid glass and iron composite cylinder was considered separately. In this case, the solution for a single cylinder was used and the phase angles of each component were added to determine the phase lag of the composite.

In order to apply the solution presented by Awbery[48] to the hollow liquid glass cylinder, a convective boundary condition was created at the outer glass surface by combining the resistance to heat transfer, r_w, of the iron crucible wall with the convection resistances , r_c, between the iron crucible and the surroundings, and a linearized radiation resistance,[40] r_r, between the crucible and the large alumina tube which contains the assembly (Figure IV.2-2). Then, the overall resistance, r_t, for the processes equals

$$r_t = r_w + \frac{1}{\frac{1}{r_c} + \frac{1}{r_r}} \qquad\qquad \text{B-1}$$

and an overall heat transfer coefficient, h, can be defined as

$$h = \frac{1}{r_T A} \qquad\qquad \text{B-2}$$

where A is the internal area of the iron crucible.

The differential equation for heat transferred radially in an infinitely long hollow circular cylinder, where the temperature, T, equals

$T(R,t)$ is

$$\frac{\partial T}{\partial t} = k \left[\frac{\partial^2 T}{\partial R^2} + \frac{1}{R}\frac{\partial T}{\partial R}\right] \qquad \text{B-3}$$

For a periodically varying temperature of amplitude, T_o, and angular frequency, ω, at the inner radius of the cylinder,

$$T(R_i,t) = T_o\, e^{(i\omega t)} \qquad \text{B-4}$$

and heat transferred by convection at the outer radius to the surroundings at T_∞.

$$-K\,\frac{\partial T(R_o,t)}{\partial R} = hA(T(R_o,t) - T_\infty) \qquad \text{B-5}$$

the solution to Equation (B-3) is

$$T(R_o,t) = A_T \cdot T_o \cdot e^{(i\omega t + \phi)} \qquad \text{B-6}$$

where the phase angle, ϕ, equals

$$\phi = \text{arc tan}\left[\frac{F(a) \cdot G(a) - F(a) \cdot G(b)}{F(a) \cdot F(b) + G(a) \cdot G(b)}\right] \qquad \text{B-7}$$

and the amplitude attenuation, A_T, equals

$$A_T = \left[\frac{F^2(b) + G^2(b)}{F^2(a) + G^2(a)}\right]^{1/2} \qquad \text{B-8}$$

The functions $F(a)$, $F(b)$, $G(a)$ and $G(b)$ are complex functions of the system size, R_i and R_o; the frequency, ω; the properties of the cylinder, k, K, ρ, and C_p; and the heat transfer coefficient, h. These relationships are presented in the notation of the computer program used to evaluate Equation (B-7). The listing of this program is presented in

Appendix B.2.

If p, a, and b are defined in the following manner

$$p = \omega/k \qquad\qquad \text{B-9a}$$

$$a = R_i p^{1/2} \qquad\qquad \text{B-9b}$$

$$b = R_o p^{1/2} \qquad\qquad \text{B-9c}$$

then

$$F(a) = \frac{1}{\rho C_p} [h\rho C_p \ (AL \cdot BN - AM \cdot BP - BL \cdot AN + BM \cdot AP)$$

$$+ kp^{1/2} \ (AM \cdot BW + AN \cdot BQ - AP \cdot BS - AL \cdot BT)] \qquad \text{B-10a}$$

$$F(b) = \frac{1}{\rho C_p} [kp^{1/2} \ (BM \cdot BW + BN \cdot BQ - BP \cdot BS - BL \cdot BT)] \quad \text{B-10b}$$

$$G(a) = \frac{1}{\rho C_p} [h\rho C_p \ (BM \cdot AN + BL \cdot AP - AM \cdot BN - AL \cdot BP)$$

$$+ kp^{1/2} \ (AM \cdot BT + AL \cdot BW - AN \cdot BS - AP \cdot BQ)] \qquad \text{B-10c}$$

$$G(b) = \frac{1}{\rho C_p} [kp^{1/2} \ (BM \cdot BT + BL \cdot BW - BN \cdot BS - BP \cdot BQ)] \quad \text{B-10d}$$

where the variables AL, AM, AN, AP, AQ, AS, AT, and AW are equal to

$$J_0 (a\sqrt{i}) = AL + i \ AM \qquad\qquad \text{B-11a}$$

$$N_0 (a\sqrt{i}) = AN + i \ AP \qquad\qquad \text{B-11b}$$

$$\sqrt{i} \ J_1 \ (a\sqrt{i}) = AQ + i \ AS \qquad\qquad \text{B-11c}$$

$$\sqrt{i} \ N_1 \ (a\sqrt{i}) = AT + i \ AW \qquad\qquad \text{B-11d}$$

and $i^2 = -1$, and $J_k(z)$ is the Bessel Function of the first kind of order k, and $N_k(z)$ is the Neumann Function of order k. By replacing a by b, AL by BL, etc., the variables BL, BM, . . . BW can be found.

To evaluate the complex Bessel Function in Equations (B-11, a through d), the Fortran IV subroutine COMBES was used, see Appendix B.3. This subroutine will evaluate the J and Y Bessel Functions of complex order and/or complex argument. To use this subroutine for Equation (B-11b) and (b-11d), the following identities were used[49]

$$N_0(z) \equiv -i\ Y_0(z) \qquad\qquad \text{B-12}$$

$$\sqrt{i}\ N_1(z) \equiv -i^{3/2}\ Y\ (z) \qquad\qquad \text{B-13}$$

The relationship between effective thermal diffusivity and phase angle of the glass cylinder was studied by evaluating Equation (B-7) for values of k between 0.010 and 0.0002 cm²/sec. The frequency range studied was from 0.005 to 0.05 Hz. The results for R_0 equal to 0.37 and 0.42 cm are shown in Figure B-1 and Figure B-2, respectively. These figures are used to interpret the results of the experimental technique.

The effect of $h\rho C_p$ on the relationship between the phase lag and k_{eff} was also investigated by computer evaluation. These results are shown in Table B-1. Because of the small dependence of the phase angle on this quantity, this effect is well within the experimental error and will not be considered further.

It was not necessary to consider "radiation slip" at the alumina-glass and iron-glass interfaces, Walther[54] has shown that for gray gasses with absorption coefficients greater than 1 cm⁻¹, the radiation slip at the

boundaries is negligible. Thus, it was assumed that there would be no slip

for the glasses used in these experiments, because their absorption coef-

ficients are much greater than one.
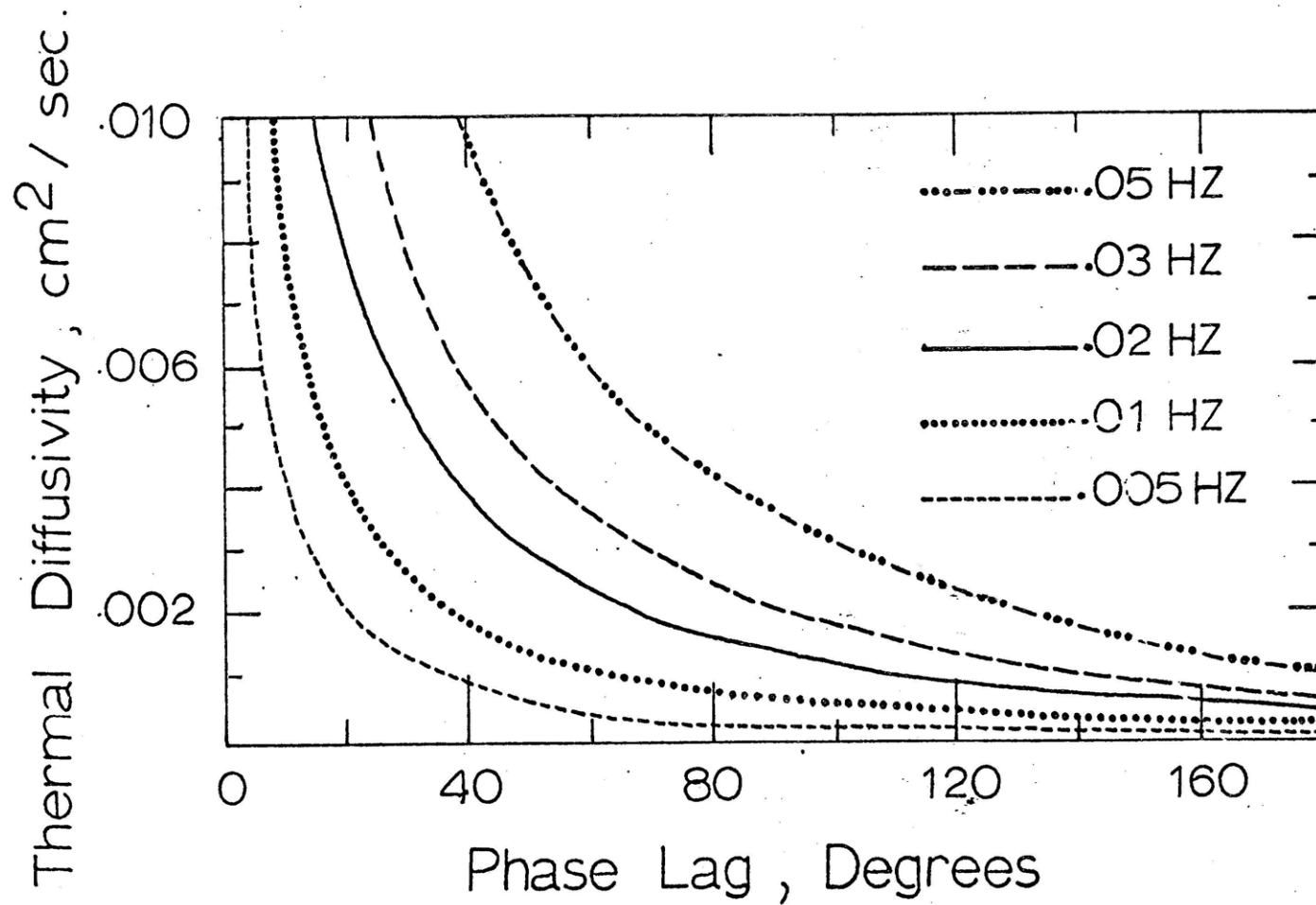
Figure B-1   Thermal diffusivity versus phase lag, calculated from Equation (B-7) for R_0 = 0.37 cm.
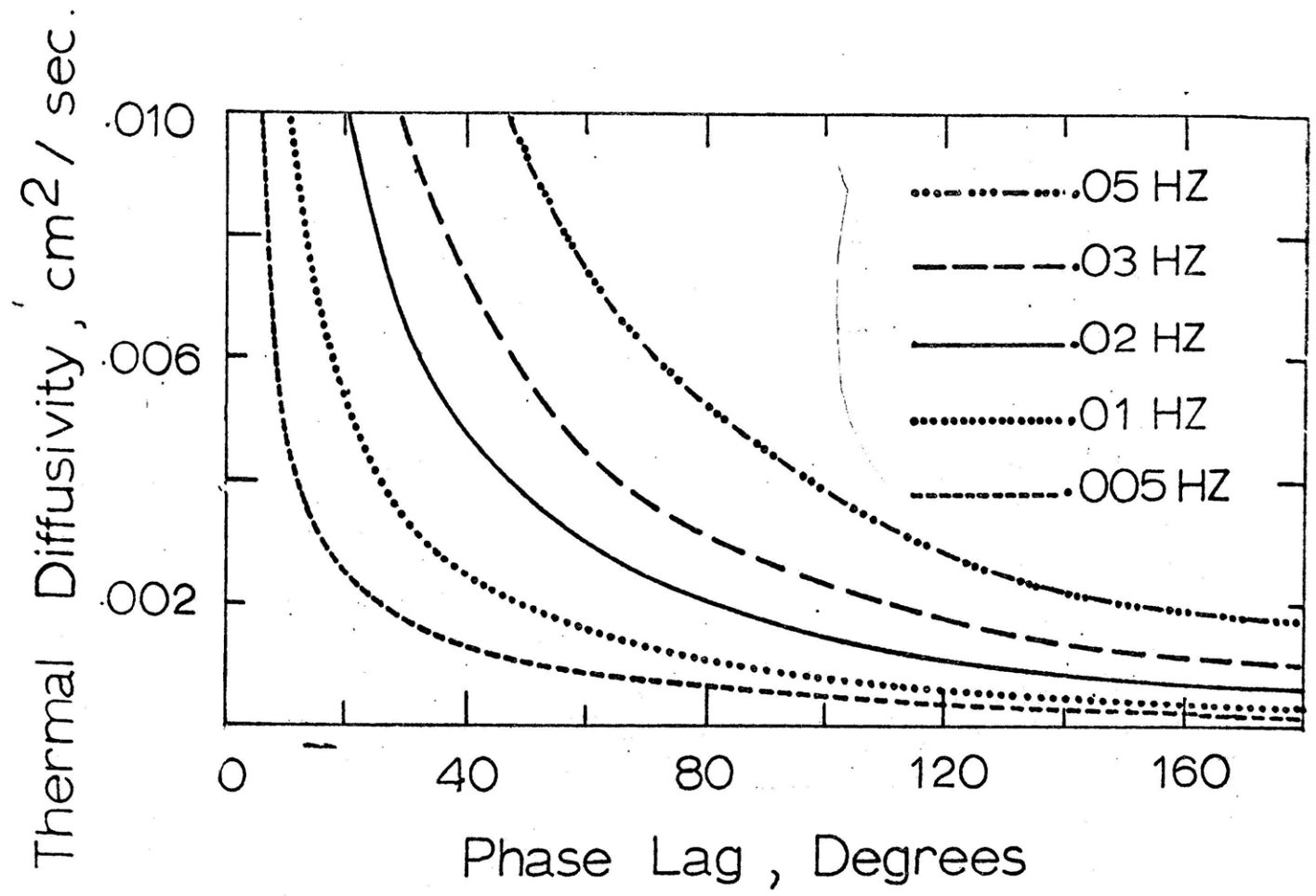
Figure B-2 Thermal diffusivity versus phase lag, calculated from Equation (B-7) for $R_0 = 0.42$ cm.

TABLE B-1

THE DEPENDENCE OF PHASE ANGLE, ϕ, ON THE QUANTITY
$h\rho C_p$ FOR R_o = 0.37 cm AND k_{eff} = 0.03 cm^2/sec

Phase Angle, ϕ

$h\rho C_p$ =	0.5	1.0	2.5	5.0
f = 0.005	11.9	11.7	11.7	11.6
f = 0.01	23.5	23.2	23.1	22.8
f = 0.03	64.5	63.9	63.6	63.0
f = 0.05	96.3	95.5	95.1	94.3

APPENDIX B.2

THE PROGRAM FOR EVALUATING THE RELATIONSHIP BETWEEN THE PHASE
ANGLE AND THE THERMAL DIFFUSIVITY, EQUATION (B-7).

```
C      ****************************************************************************
C
C      PROGRAM TO CALCULATE THE PHASE LAG, PHI, BETWEEN A SINUSOIDAL TEMPERATURE
C      AT THE INNER RADIUS, RI, AND THE RESPONSE AT THE OUTER RADIUS, RO, OF A
C      HOLLOW CIRCULAR CYLINDER.  PHI IS FOUND FOR SPECIFIED VALUES OF THE
C      EFFECTIVE THERMAL DIFFUSIVITY, ALPA, FREQUENCY, FREQ, AND E, THE HEAT
C      TRANSFER COEFFICIENT AT RO, DIVIDED BY THE DENSITY TIMES THE HEAT CAPACITY
C      OF THE CYLINDER.
C
C
C      ****************************************************************************
C
       DIMENSION BJRE(50),BJIM(50),BYRE(10),BYIM(10)
       DIMENSION TANPHI(50),PHI(50,10),E(10)
     1 READ (5,2) RI,RO,FREQ
     2 FORMAT (3F12.6)
       WRITE (6,3) RI,RO,FREQ
     3 FORMAT ('1      THE RESULTS FOR RI = ',F7.5,' CM. , RO = ',F7.5, ' CM. , AND
      1M. , AND FREQ = ',F6.4,' HZ. .')
       E(1) = 0.25
       E(2) = 0.5
       E(3) = 0.75
       E(4) = 1.0
       F(5) = 2.5
       E(6) = 5.0
       WRITE (6,4) (E(M),M=1,6)
     4 FORMAT (//,7X,'ALPA',7X,'E = ',4X,F5.3,8F12.3)
       DO 10 I=1,50
       ALPA = 0.010 - 0.0002 * ( I-1 )
       PHI(I,1) = ALPA
       A=RI*SQRT(6.28318*FREQ/ALPA)
       B=RO*SQRT(6.28318*FREQ/ALPA)
       D = SQRT(6.28318*FREQ*ALPA)
       AX = A/SQRT(2.0)
       AY = A/SQRT(2.0)
C
C      ****************************************************************************
```

```
C
C      COMBES IS AN IPC SUPPLIED SUBROUTINE, WHICH CALCULATES THE J AND Y BESSEL
C      FUNCTIONS OF REAL AND COMPLEX ORDER, OF REAL AND COMPLEX ARGUEMENTS.
C      FOR MORE INFORMATION, SEE IPC PUBLICATION AP - 14.
C
C      ****** ** * ****************************************************************
C
       CALL COMBES (AX,AY,0.0,0.0,1,BJRE,BJIM,BYRE,BYIM)
       AL = BJRE(1)
       AM = BJIM(1)
       AN = BYIM(1)
       AP = -BYRE(1)
       AQ = (BJRE(2)-BJIM(2))/SQRT(2.0)
       AS = (BJRE(2)+BJIM(2))/SQRT(2.0)
       AT = (BYRE(2)+BYIM(2))/SQRT(2.0)
       AW = -(BYRE(2)-BYIM(2))/SQRT(2.0)
       BX = B/SQRT(2.0)
       BY = B/SQRT(2.0)
       CALL COMBES (BX,BY,0.0,0.0,1,BJRE,BJIM,BYRE,BYIM)
       BL = BJRE(1)
       BM = BJIM(1)
       BN = BYIM(1)
       BP = -BYRE(1)
       BQ = (BJRE(2)-BJIM(2))/SQRT(2.0)
       BS = (BJRE(2)+BJIM(2))/SQRT(2.0)
       BT = (BYRE(2)+BYIM(2))/SQRT(2.0)
       BW = -(BYRE(2)-BYIM(2))/SQRT(2.0)
       C1 = AL*BN-AM*BP-AN*BL+AP*BM
       C2 = AM*BW+AN*BQ-AP*BS-AL*BT
       C3 = BM*BW+BN*BQ-BP*BS-BL*BT
       C4 = AN*BM+AP*BL-AM*BN-AL*BP
       C5 = AM*BT+AL*BW-AN*BS-AP*BQ
       C6 = BM*BT+BL*BW-BN*BS-BP*BQ
       D1=C3*C4-C1*C6
       D2=(C3*C5-C2*C6)*D
       D3=C1*C3+C4*C6
```

```
      D4=(C2*C3+C5*C6)*D
      DO 20 J=1,6
      K = J + 1
      EE = E(J)
      TANPHI(J) = (D1+D2/EE)/(D3+D4/EE)
      IF (TANPHI(J) .GT. 6000.0) GO TO 18
      IF (TANPHI(J) .LT. -6000.0) GO TO 19
      PHI(I,K) = ATAN ( TANPHI(J))*180.0/3.14159
      GO TO 20
   18 PHI(I,K) = 90.0
      GO TO 20
   19 PHI(I,K) = -90.0
   20 CONTINUE
      WRITE (6,21) ALPA, (PHI(I,L),L=1,6)
   21 FORMAT ('0      ',F6.4,5X,6F12.2)
   10 CONTINUE
      GO TO 1
      END
```

APPENDIX B.3

COMBES, A FORTRAN IV SUBROUTINE FOR
EVALUATING COMPLEX BESSEL FUNCTIONS

MASSACHUSETTS INSTITUTE OF TECHNOLOGY
INFORMATION PROCESSING CENTER
Applications Development Group

December 4, 1969

NAME: Complex Bessel (COMBES)

DESCRIPTION: COMBES is a set of 17 FORTRAN IV subroutines that
                compute the values of J and Y Bessel functions for
                complex values of the argument and order. Because
                FORTRAN complex arithmetic is not used, complex
                inputs to COMBES are given in two parts, real and
                imaginary. COMBES cannot be used conveniently to
                compute solutions to the I and K Bessel functions.
                The programmer is urged to use subroutines BESI
                and BESK in IBM's Scientific Subroutine Package (SSP)
                for this purpose.

USAGE: The calling sequence for COMBES is:

                CALL COMBES(X,Y,ALPHA,BETA,N,BJRE,BJIM,BYRE,BYIM)

                Where:

                X   is the real part of the argument.

                Y   is the imaginary part of the argument.

                BJRE and   are one-dimensional arrays containing
                BJIM   the real and imaginary parts of the
                                solutions of the J Bessel function
                                for argument (X,Y) and a range of
                                orders defined by ALPHA, BETA and N
                                (see below). BJRE and BJIM should be
                                dimensioned as described for N.

                BYRE and   are one-dimensional arrays containing
                BYIM   the real and imaginary parts of the
                                solutions for the Y Bessel function
                                for argument (X,Y) and a range of
                                orders from (ALPHA,BETA) to
                                (ALPHA+N,BETA). BYRE and BYIM must
                                be dimensioned at least N+1.

$$\left[BYRE(1)+iBYIM(1) = Y_{\eta_1}(X+iY), \dots, \right.$$

$$BYRE(N+1)+iBYIM(N+1) = Y_{\eta_{n+1}}(X+iY) \text{ where}$$

$$\eta_1 = ALPHA+iBETA, \quad \eta_{n+1} = (ALPHA+N)+iBETA \Big]$$

N   The significance of N for the Y   106
       Bessel function is described
       under BYRE and BYIM. For the
       J Bessel function, N is used to
       compute a quantity K as follows:

KTEN = 20.0 + SQRT(X**2 + Y**2)
M   = MAX0(KTEN,IABS(N)+10)/2
K   = 2*M + 1

Where X and Y are the X and Y in the calling
sequence of COMBES. Then K values of the
J Bessel function are computed, corresponding
to orders ALPHA+iBETA up to ALPHA+(K-1)+iBETA.
BJRE and BJIM must be dimensioned at least K+2.
N is a fixed-point variable.

$$\big[BJRE(1)+iBJIM(1) = J_{n_1}(X+iY),\ldots,$$

$$BJRE(K)+iBJIM(K) = J_{n_K} = (X+iY)\text{ where}$$

$$n_1 = ALPHA+iBETA,\ n_K = ALPHA+(K-1)+iBETA\big]$$

ALPHA   is the minimum of the real parts of
           the orders for which the J and Y
           Bessel functions are to be computed.
           Restrictions on ALPHA are listed
           below. ALPHA is floating point.

BETA   is the imaginary part of all the
           orders used by COMBES. BETA is
           floating point.

RESTRICTION: ALPHA has one restriction. In order to get accurate
               results for the Y Bessel function, the following con-
               dition must be satisfied: either BETA $\neq$ 0.0 or ALPHA $\neq$
               n where n is a positive integer equal to or less than
               (K-5)/2. If this condition is not satisfied, the J
               values will be accurate, although divide check inter-
               rupts will occur during computation of the Y function.

TIMING AND   COMBES is fast compared to the time required for
ACCURACY: SSP routines BESJ and BESY to compute comparable
               results if solutions for a range of orders are
               desired. However, for a single (real) value of
               the order, BESJ and BESY are faster than COMBES
               and may be more accurate. In general, COMBES and
               BESJ produce similar results. For values of the
               argument greater than 10.0, BESY appears to be
               more accurate than COMBES.

The following tables correspond to Y=0.0 and ALPHA=BETA=0.0.

For the J function:

Values of X	Range of order	Precision
X = 5.0	≤ 20	five significant digits (± 5 in sixth digit)
X = 10.0	< 20	five significant digits
X = 15.0	≤ 11	four or five significant digits
X = 20.0	< 11	same
X = 50.0	≤ 20	four significant digits
X = 100.0	≤ 20	same

For the Y function:

Values of X	Range of order	Precision
X = 5.0	< 20	five significant digits
X = 10.0	≤ 20	five significant digits with two exceptions. Order 0 gives only four digits, order 8 gives only three digits. In each case BESY gives one more digit of precision.
X = 15.0	≤ 10	three to six significant digits. For orders 3 and 9, COMBES gives only three digits. BESY gives five significant digits over the entire range.
X = 20.0	≤ 10	five significant digits
X = 50.0	≤ 20	four significant digits; BESY gives 5.
X = 100.0	≤ 20	same

The accuracy of COMBES, BESJ and BESY was tested against the tables on pages 390 to 408 in the Handbook of Mathematical Functions, edited by Abramowitz and Stegun. Because of a lack of appropriate tables, the accuracy of COMBES for complex orders could not be tested adequately.

AVAILABILITY: COMBES is available in load module form in the library SYS5.MATHLIB.SUBR and in source form in SYS5.MATHLIB.SOURCE. For further information about the use of these libraries, refer to APR-2 or consult the Programming Assistants, Room 39-219.

CORE
REQUIREMENT: The entire COMBES package (17 subroutines) requires
16,952 bytes of core storage (4238 bytes in hexa-
decimal).

REFERENCES: COMBES was originally written in FORTRAN II by
Max Goldstein at New York University. The con-
version to FORTRAN IV was performed by the Computa-
tion Group of the M.I.T. Research Laboratory of
Electronics.

Abramowitz, Milton and Irene A. Stegun (editors).
Handbook of Mathematical Functions with Formulas,
Graphs, and Mathematical Tables, National Bureau
of Standards, Applied Mathematics Series 55, August,
1966.

BIBLIOGRAPHY

1. R. Siegel and J.R. Howell: Thermal Radiation Heat Transfer, McGraw-Hill Book Company, New, York, 1972.

2. B.S. Kellett: "Steady Flow of Heat Through Hot Glass", J. Opt. Soc. Amer., 1952, Vol. 42, pp. 339-343.

3. M. Czerny and L. Genzel: "Energy Flux and Temperature Distribution in Glass Baths of Melting Tanks Resulting from Conduction and Radiation", Glastech. Ber., 1952, Vol. 25, pp. 387-392.

4. W. Geffcken: "Transmission of Heat in Glass at High Temperatures", Glastech. Ber., 1952, Vol. 25, pp. 392-396.

5. L. Genzel: "Calculation of the Radiation Conductivity of Glasses", Glastech. Ber., 1953, Vol. 26, pp. 69-71.

6. M. Czerny, L. Genzel, and G. Heilmann: "Radiation Flux Inside Glass Tanks", Glastech. Ber., 1955, Vol. 28, pp. 185-190.

7. H. Charnock: "Experimental and Theoretical Comparison of Radiation Conductivity Predicted by Steady-State Theory With That Effective Under Periodic Temperature Conditions", J. Amer. Cer. Soc., 1961, Vol. 44, pp. 313-317.

8. R. Gardon: "A Review of Radiant Heat Transfer in Glass", J. Amer. Cer. Soc., 1961, Vol. 44, pp. 305-312.

9. T. Smith: "Note on Measurements of Glass Absorption", Proc. Phys. Soc. (London), 1946, Vol. 58, pp. 472-475.

10. L. Genzel: "Measurement of the Infrared Absorption of Glass Between 20° and 1360°C", Glastech. Ber., 1951, Vol. 24, pp. 56-63.

11. F.J. Grove: "Spectral Transmission of Glass at High Temperature and Its Application to Heat Transfer Problems:, J. Amer. Cer. Soc., 1961, Vol. 44, pp. 317-320.

12. M. Coenen: "Transmission of Radiation in the Colored Glass Bath", Glastech. Ber., 1968, Vol. 41, pp. 1-10.

13. W.A. Weyl: Colored Glasses, Soc. of Glass Technology, Sheffield, England, 1951.

14. P. Acloque: "Some Methods of Measuring Thermal Conductivity of Glass", Verres et Réfractaires, 1959, Vol. 13, No. 3, pp. 131-42, No. 4, 191-203, No. 5, 239-252.

15. R.D. Cowan: "Proposed Method of Measuring Absorption Coefficient at High Temperatures", J. of Appl. Phys., 1961, Vol. 32, pp. 1363-70.

16. M. Bre and P. Kermabon: "Thermal Diffusivity of Some Industrial Glasses at High Temperatures", Verres Refract., 1969, Vol. 23, pp. 3-9.

17. A.F. VanZee and C.L. Babcock: "Method for the Measurement of Thermal Diffusivity of Molten Glass", J. Amer. Cer. Soc., 1951, Vol. 34, pp. 244-250.

18. E.F. Sevast'yanow and A.A. Sokolov: "Study of Thermophysical and Electrical Parameters of the Transfer of Heat and Electicity in Molten Glass: I, Unit for Complex Study of Effective Coefficient of Radiant-Molecular Heat Conductivity and Volume Resistivity of the Molten Glass", Steklo, Trudy Inst. Stekla, 1966, No. 2, pp. 80-84.

19. N.D. Eryou and L.R. Glicksman: "An Experimental and Analytical Study of Radiative and Conductive Heat Transfer in Molten Glasses", J. Heat Trans., 1972, Vol. 94, pp. 224-234. From M.S. Thesis by K.H.Chen, M.I.T.

20. Y.S. Touloukian: Thermo-Physical Properties of High Temperature Solid Materials, Vol. 4, McMillan Company, New York, 1967.

21. F.J. Grove and P.E. Jellyman: "Infrared Transmission of Glass in the Range Room Temperature to 1400°", J. Soc. Glass Technol., 1955, Vol. 39, pp. 3-15

22. H. Carson and J. Chipman: "Oxygen Activity in Iron Oxide Slags", Trans. AIME, 1953, Vol. 197, pp. 1089-1096.

23. J.F. Elliott, M. Gleiser and V. Ramakrishna: Thermochemistry for Steelmaking, Vol. II, Addison-Wesley Publishing Company, Inc., Reading, Massachusetts, 1963.

24. Professor D. Uhlmann: private communication.

25. Y. Beers: Introduction to the Theory of Error, Addison-Wesley Publishing Company, Reading, Massachusetts, 1957.

26. T. Engh: private communication.

27. W.M. Rohsenow and C.Y. Choi: Heat, Mass and Momentum Transfer, Prentice-Hall, Inc., Englewood Cliffs, New Jersey, 1961.

28. W.D. Kingery: "Heat Conductivity Processes in Glass", J. Amer. Cer. Soc., 1961, Vol. 44, pp. 302-304.

29. C. Kittel: "Interpretation of the Thermal Conductivity of Glasses", Physical Review, 1949, Vol. 75, pp. 972-974.

30. W.D. Kingery: "The Thermal Conductivity of Ceramic Dielectrics", Progress in Ceramic Science, Vol. 2, Pergamon Press, London, 1961.

31. K.L. Wray and T.J. Connolly: "Thermal Conductivity of Clear Fused Silica at High Temperatures", J. App. Phys., 1959, Vol. 30, pp. 1702-1705.

32. C. Diaz: Compilation of the Properties of Copper Smelting Slags, private communication.

33. C.R. Masson: "Thermodynamics and Constitution of Silicate Slags", J. Iron and Steel Inst., 1972, Vol. 210, pp. 89-96.

34. G. Derge: Basic Open Hearth Steelmaking, 3rd Ed., AIME, New York, 1964.

35. E.H. Ratcliffe: "A Survey of Most Probable Valves for the Thermal Conductivities of Glasses Between About -150 and 100°C, Including New Data on Twenty-Two Glasses and a Working Formula for the Calculation of Conductivity from Composition", J. of Glass Technol., 1963, Vol. 4, pp. 113-128.

36. R.C. Weast: Handbook of Chemistry and Physics, 52nd Ed., Chemical Rubber Company, Cleveland, Ohio, 1971.

37. M. Kunugi, S. Tanaka, S. Shimizu, and K. Kitamura: "Heat Transmission Through Molten Glass", J. Cer. Assoc., Japan, 1954, Vol. 62, pp. 780-784.

38. F.N. Steele and R.W. Douglas: "Observations on the Absorption of Iron in Silicate and Borate Glasses", Phys. Chem. Glasses, 1965, Vol. 6, pp. 246-252.

39. P.V. Danckwerts: "Significance of Liquid-Film Coefficients in Gas Absorption", Ind. Eng. Chem., 1951, Vol. 43, p. 1460-1467.

40. R. Schuhmann: Metallurgical Engineering, Engineering Principles, Vol. 1, Addison-Wesley Publishing Company, Inc., Reading, Massachusetts, 1952.

41. P.J. Yavorsky: Ph.D. Thesis, Massachusetts Institute of Technology, Cambridge, Massachusetts, 1970.

42. C.E. Sims: Electric Furnace Steelmaking, Design, Operation, and Practice, Vol. 1, 2nd Ed., AIME, New York, 1967.

43. Professor J.F. Elliott: private communication

44. Professor J.F. Elliott: Private communication

45. M. Hansen: <u>Constitution of Binary Alloys</u>, 2nd Ed., McGraw-Hill Book Company, Inc., New York, 1958.

46. G.M. Bigger: "Molybdenum as a Container for Melts Containing Iron Oxide", <u>Ceram. Bull.</u>, 1970, Vol. 49, pp. 286-288.

47. H.S. Carslaw and J.C. Jaeger: <u>Conduction of Heat in Solids</u>, 2nd Ed. Oxford University Press, Ely House, London, 1959.

48. J.H. Awbery: "The Periodic Flow of Heat in a Hollow Cylinder", <u>Phil. Mag.</u>, 1939, Vol. 28, pp. 447-451.

49. F.B. Hildebrand: <u>Advanced Calculus for Applications</u>, Prentice-Hall, Inc., Englewood Cliffs, New Jersey, 1962.

50. T. Lyman: <u>Metals Handbook, Properties and Selection of Metals</u>, Vol. 1, ASM, Metals Park, Ohio, 1961.

51. G. Johnston: private communication.

52. Professor L.R. Glicksman: private communication.

53. J. Bockris, J. White and J. MacKenzie: <u>Physiochemical Measurements at High Temperatures</u>, Academic Press, New York, 1959.

54. A. Walther, J. Dorr, and E. Eller: "Mathematical Calculation of Temperature Distribution in a Glass Melt Due to Heat Conduction and Radiation", <u>Glastech. Ber.</u>, 1953, Vol. 26, pp. 133-40.

BIOGRAPHICAL NOTE

The author was born on June 5, 1948, in Brooklyn, New York. He attended the public schools of Broward County, Florida, and graduated with honors from the Bolles School of Jacksonville, Florida.

The author attended Carnegie-Mellon University where he received the degrees of Bachelor of Science and Master of Science in Metallurgy and Materials Science in June, 1969. After leaving Carnegie-Mellon University, the author studied at the Massachusetts Institute of Technology. He received the degree of Doctor of Science in Metallurgy and Materials Science in June, 1973.

The author is a member of the Sigma Xi Honorary, The American Institute of Mining, Metallurgical and Petroleum Engineers and the American Society for Metals.

The author is happily married and has no children.